AD-A092 910 MICHIGAN STATE UNIV EAST LANSING DEPT OF ASTRONOMY A--ETC F/G 3/2
SOLAR ATMOSPHERIC DYNAMICS.(U)
MAY 80 R F STEIN F19628-77-C-0068
UNCLASSIFIED AFGL-TR-80-0208 NL

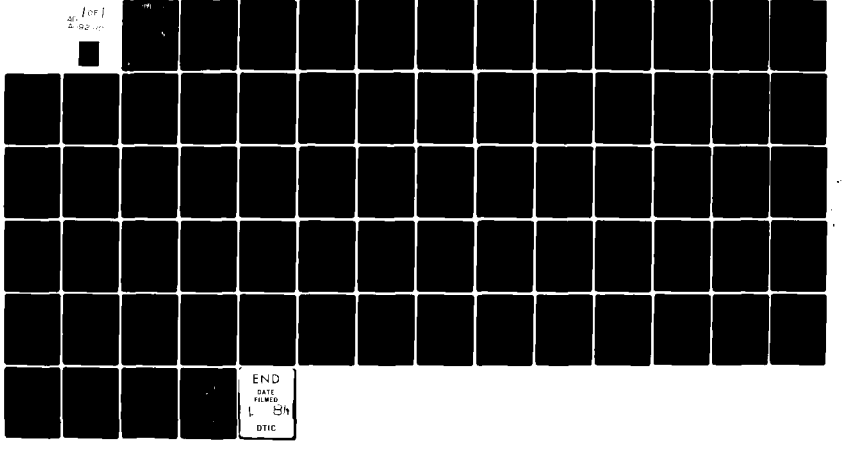

END
DATE FILMED
1 81
DTIC

AFGL-TR-80-0208

SOLAR ATMOSPHERIC DYNAMICS

by

Robert F. Stein

Department of Astronomy and Astrophysics

Michigan State University

East Lansing, MI 48824

May 1980

Final Scientific Report

1 March 1977 - 30 September 1979

Approved for public release; distribution unlimited

Air Force Geophysics Laboratory

Air Force Systems Command

United States Air Force

Hanscom AFB, Massachusetts 01731

UNCLASSIFIED
SECURITY CLASSIFICATION OF THIS PAGE (When Data Entered)

REPORT DOCUMENTATION PAGE

READ INSTRUCTIONS BEFORE COMPLETING FORM

1. REPORT NUMBER: AFGL-TR-80-0208	2. GOVT ACCESSION NO.: AD-A092 910
3. RECIPIENT'S CATALOG NUMBER:	
4. TITLE (and Subtitle): SOLAR ATMOSPHERIC DYNAMICS.	5. TYPE OF REPORT & PERIOD COVERED: Final ~~Scientific~~ Report. 1 March 77-30 Sept~~ember~~ 79
	6. ~~PERFORMING ORG. REPORT NUMBER~~
7. AUTHOR(s): Robert F. Stein	8. CONTRACT OR GRANT NUMBER(s): F19628-77-C-0068
9. PERFORMING ORGANIZATION NAME AND ADDRESS: Department of Astronomy and Astrophysics, Michigan State University, East Lansing, MI 48824	10. PROGRAM ELEMENT, PROJECT, TASK AREA & WORK UNIT NUMBERS: 61102F, 2311G3AG
11. CONTROLLING OFFICE NAME AND ADDRESS: Air Force Geophysics Laboratory, Hanscom AFB, Massachusetts 01731, Monitor/Richard Altrock/PH	12. REPORT DATE: May 1980
	13. ~~NUMBER OF PAGES~~: 70
14. MONITORING AGENCY NAME & ADDRESS (if different from Controlling Office)	15. SECURITY CLASS. (of this report): UNCLASSIFIED
	15a. DECLASSIFICATION DOWNGRADING SCHEDULE

16. DISTRIBUTION STATEMENT (of this Report)

Approved for public release; distribution unlimited

17. DISTRIBUTION STATEMENT (of the abstract entered in Block 20, if different from Report)

18. SUPPLEMENTARY NOTES

19. KEY WORDS (Continue on reverse side if necessary and identify by block number)

Radiative Shock Dynamics
Magneto-Acoustic-Gravity Waves
"Modal" Fluid Dynamic Calculations"
Solar Chromospheric Heating

20. ABSTRACT (Continue on reverse side if necessary and identify by block number)

We have studied the heating of the solar chromosphere and transition region by acoustic waves. We find they are incapable of transporting sufficient energy through the chromosphere to heat the transition region and corona. We are developing a radiative fluid dynamic computer code to study acoustic heating of the chromosphere and the effect of acoustic waves on line profiles. In order to study heating by other types of wave motions we have analyzed the wave vector surface of the Magneto-Acoustic-Gravity Waves and are developing a "modal" computer code to study their propagation and dissipation.

DD FORM 1 JAN 73 1473 EDITION OF 1 NOV 65 IS OBSOLETE

UNCLASSIFIED
SECURITY CLASSIFICATION OF THIS PAGE (When Data Entered)

SOLAR ATMOSPHERIC DYNAMICS

I. INTRODUCTION

The goal of this research is to study solar atmospheric waves and their role in heating the chromosphere and corona. To this end we are calculating the propagation of radiating acoustic shock waves and their effect on solar spectral lines. The ability of acoustic waves to heat the corona has been cast into doubt because they are not observed to carry sufficient energy into the transition region and because the corona is observed to consist of magnetic flux tubes. To clarify this issue we have made detailed theoretical studies of acoustic wave flux and heating of the chromosphere and are developing a "modal" code to calculate magnetic type wave propagation. As a preliminary step we have studied the wave vector surface of Magneto-Acoustic-Gravity Waves.

II. RADIATIVE SHOCK DYNAMICS

The development of computer codes to study radiating shocks was begun. These programs will be applied to study the heating of solar and stellar chromospheres by acoustic waves and the detailed analysis of spectral line profiles in the presence of acoustic waves. The first stage in this project was the development of a grey-LTE-continuum radiation hydradynamic code, which is described below.

The dynamics is determined by the equations of mass and momentum conservation.

Conservation of Mass:

$$\frac{\partial R}{\partial m} = \frac{1}{\rho},$$

where m is the mass column density of position R.

Conservation of Momentum:

$$\frac{\partial U}{\partial t} = -\frac{\partial}{\partial m}(P + Q) - g,$$

where Q is an artifical viscosity to stabilize the numerical calculations.

$$Q = \begin{cases} \rho \left(\frac{\partial U}{\partial x}\right)^2 \ell^2 & \text{if } \frac{\partial U}{\partial x} < 0 \\ 0 & \text{otherwise} \end{cases}$$

where ℓ is a constant with the dimensions of a length.

Velocity U and position R are related by

$$\frac{\partial R}{\partial t} = U.$$

These equations are solved by dividing the atmosphere into layers of given mass column density $\Delta m_{j+1/2} = m_{j+1} - m_j$; and transforming the differential equations into finite difference equations on this Lagrangian grid (Christy, 1964; Richtmyer and Morton, 1967).

The velocity $U_j^{n+1/2}$ and position P_j^n are defined at the zone boundaries, with the velocity at the half integral times $t^{n+1/2} = t^n + 1/2\ \Delta t$ and the position at the integral times t^n. All the other variables are defined at

the zone centers j+1/2 and integral times t^n. The finite difference equations are solved explicitly for $U_j^{n+1/2}$, then R_j^{n+1}, then $\rho_{j+1/2}^{n+1}$, and finally $Q_{j+1/2}^{n+1/2}$ by making a sweep through the grid and solving the finite difference equations in the following order:

First solve

$$\frac{U_j^{n+1/2} - U_j^{n-1/2}}{\Delta t^n} = -g - \frac{P^n_{j+1/2} - P^n_{j-1/2} + Q^{n-1/2}_{j+1/2} - Q^{n-1/2}_{j-1/2}}{\Delta m_j}$$

for the velocity $U_j^{n+1/2}$, j = 2, ..., N-1, where $\Delta m_j = 1/2\ (\Delta m_{j+1/2} + \Delta m_{j-1/2})$ and $\Delta m_{j+1/2} = m_{j+1} - m_j$ and $\Delta t^n = 1/2\ (\Delta t^{n+1/2} + \Delta t^{n-1/2})$ and $\Delta t^{n+1/2} = t^{n+1} - t^n$.

Second solve

$$\frac{R_j^{n+1} - R_j^n}{\Delta t^{n+1/2}} = U_j^{n+1/2}$$

for the position of the zone boundaries R_j^{n+1}, j = 1, ..., N. Third solve

$$\frac{R_{j+1}^{n+1} - R_j^{n+1}}{\Delta m_{j+1/2}} = \frac{1}{\rho}^{n+1}_{j+1/2}$$

for the density $\rho_{j+1/2}^{n+1}$ j = 1, ..., N-1. Finally calculate the new artificial viscosity

$$Q_{j+1/2}^{n+1/2} = \alpha\ 1/2\ (\rho_{j+1/2}^{n+1} + \rho_{j+1/2}^{n})\ (U_{j+1}^{n+1/2} - U_j^{n+1/2})^2,$$

when $\rho_{j+1/2}^{n+1} > \rho_{j+1/2}^{n}$

= 0 otherwise.

We take $\alpha = 2$. The velocity must be specified at the two boundaries. We use a piston at the lower boundary

$$U_1^{n+1/2} = A\sin(\omega t^{n+1/2}),$$

and a transmitting upper boundary

$$U_N^{n+1/2} = U_N^{n-1/2} + (U_{N-1}^{n-1/2} - U_N^{n-1/2})\ S_{N-1/2}^n\ \Delta t^n / (R_N^n - R_{N-1}^n)$$

where $S = \sqrt{\gamma P/\rho}$ is the sound speed.

The thermodynamics is determined by the equations of energy conservation, radiative transfer, and LTE ionization.

Energy conservation:

$$\frac{\partial E}{\partial t} + (P+Q)\frac{\partial}{\partial t}\left(\frac{1}{\rho}\right) = 4\pi \mathcal{H}\ (J-B) - \frac{\partial F}{\partial m}$$

where $E = 3/2\ nkT/\rho + x\chi_H/\bar{m}$ is the thermal plus ionization energy per unit mass, and n is the total particle density, x is the fractional ionization, χ is the ionization potential and $\bar{m}$ is the mean mass per particle. The conductive flux is $F = 7.6 \times 10^{-7} T^{5/2} \frac{dT}{dZ}$

Transfer equation:

$$\mu^2 \frac{\partial}{\partial m}\left[\frac{1}{\kappa+\sigma}\right]\frac{\partial J}{\partial m} = \kappa\ (J-B)$$

where κ is the absorption opacity and σ is the scattering opacity, and $\mu^2 = 1/3$.

Saha equation:

$$\frac{x(x+fA)}{1-x} = \phi(T) = \frac{K}{\bar{m}} T^{3/2} \rho^{-1} e^{-\chi/kT}$$

where K = 0.333368 for hydrogen and fA is the fraction of electrons from heavier elements (assumed fixed).

These equations are solved in finite difference form on the same grid as the dynamics, implicitly and simultaneously be Newton-Raphson itleration (complete linearization). The finite difference equations are:

Energy:

$$E^{n+1}_{j+1/2} - E^{n}_{j+1/2} + \left[P^{n+1}_{j+1/2} + Q^{n+1/2}_{j+1/2}\right]\left(\frac{1}{\rho^{n+1}_{j+1/2}} - \frac{1}{\rho^{n}_{j+1/2}}\right)$$

$$- H^{n+1}_{j+1/2}\ \Delta t^{n+1/2} = 0,$$

where the heat input is $H_{j+1/2} = 4\pi \kappa_{j+1/2} (J_{j+1/2} - B_{j+1/2}) - \frac{F_{j+1} - F_j}{\Delta m_{j+1/2}}$,

and the conductive flux is

$$F_j = - C.1/2 \, (x_{j+1/2} + x_{j-1/2}) \frac{\rho_{j+1/2} + \rho_{j-1/2}}{\Delta m_{j+1/2} + \Delta m_{j-1/2}}$$

$$\left(\frac{T_{j+1/2} + T_{j-1/2}}{2}\right)^{5/2} (T_{j+1/2} - T_{j-1/2}).$$

The boundary conditions on the flux are that C = 0 below the temperature minimum and $F_{N-1} = 0$ or $T_{N-3/2} = T_{N-1/2}$ at the upper boundary.

The number density of particles is

$$n = n_H \{1+x+B+A(1+f)\}$$
$$= \rho \{1+x+B+A(1+f)\} / m_H (1+4B+w)$$
$$= \rho \{1+x+B+A(1+f)\} / \bar{m}$$

where B is the ratio of helium to hydrogen by number, A is the ratio of heavier elements to hydrogen by number, w is the mean atomic weight of the heavy elements times A, and f is the fraction of electrons from heavy elements. The total internal energy per unit mass is

$$E = E_{th} + E_{ion}$$
$$E_{th} = 3/2 \frac{k}{\bar{m}} T \{1+x+B+A(1+f)\}$$
$$E_{ion} = \frac{k}{\bar{m}} T_{ion} x, \; T_{ion} = \frac{\chi}{k} = 1.58 \times 10^5 \, ^oK$$

Transfer:

$$\frac{J_{j+3/2} - J_{j+1/2}}{\Delta\tau_{j+1}} - \frac{J_{j+1/2} - J_{j-1/2}}{\Delta\tau_j} - \frac{\Delta\tau_{j+1/2}}{2} (J_{j+1/2} - B_{j+1/2}) = 0$$

where $\Delta\tau_{j+1/2} = \kappa_{j+1/2} \, \Delta m_{j+1/2}$

$$\Delta\tau_j = 1/2 \, (\Delta\tau_{j+1/2} + \Delta\tau_{j-1/2})$$

$\mu^2 = 1/3$

$\kappa = \kappa(\rho, T)$ from table

$B = \frac{\sigma}{\pi} T^4$

The upper boundary condition on the radiation field is no incident radiation, so

$$\frac{J_{N-1/2} - J_{N-3/2}}{\Delta\tau_{N-1}} = -1/2\,(J_{N-1/2} + J_{N-3/2}) + B_{N-1/2}\,\Delta\tau_{N-1/2}.$$

The lower boundary condition is

$$J_{3/2} = B_{3/2}$$

that is an adiabatic first layer.

Saha:

$$X^{n+1}_{j+1/2} - 2\phi / \{\phi + Af + (4\phi + Af)^2 + 4\phi\} = 0$$

where $\phi = K\,(k/\bar{m})\,\rho^{-1}\,T^{3/2}\exp(\chi/kT)$

and $K = 0.333368$, $\chi/k = 1.58 \times 10^5\ ^oK$.

These three equations are solved by linearizing them in the corrections δT, δJ, and δx, and solving the resulting block tri-diagonal system for these corrections.

After the new temperature distribution is obtained, the Saha and transfer equations are solved for the ionization x and mean intensity J consistent with that temperature distribution. The formal solution of the transfer equation involves sums of large terms $(\Delta\tau)^{-1}$ and small terms $(\Delta\tau)$ at small optical depth and in the usual tri-diagonal Gaussian elimination scheme all significance would be lost. Therefore to be able to carry the calculations out to optical depths as small as the smallest machine floating point number the elimination scheme was modified as follows: The transfer equation has the form

$$A_i\,J_{i-1} + B_i\,J_i + C_i\,J_{i+1} = D_i.$$

The usual procedure is to calculate elimination matrices

$$E_{i+1} = (B_i + A_i\,E_{i-1})^{-1}C_i \text{ and } F_{i+1} = -(B_i + A_i\,E_{i-1})^{-1}\,(D_i + A_i\,F_{i-1}),$$

where these are then used to back substitute for the

$$J_i = E_i\,J_{i+1} + F_i.$$

At small optical depth the radiation field is nearly constant and E_i nearly the identity matrix 1. It is therefore possible to gain accuracy by working with a matrix ϵ_i equal to the difference between E_i and 1.

That is, let

$$\epsilon_i = 1 - E_i$$

$$J_i = (1 - \epsilon_i) J_{i+1} + F_i$$

The relations to calculate ϵ_i and F_i are found by substituting this equation into the difference equation. The result is

$$\epsilon_i = \left(B_i + A_i - A_i \epsilon_{i-1} \right)^{-1} \left(B_i + A_i + C_i - A_i \epsilon_{i-1} \right)$$

$$F_i = \left(B_i + A_i - A_i \epsilon_{i-1} \right)^{-1} \left(D_i + A_i F_{i-1} \right)$$

The large terms in the sum $B_i + A_i + C_i$ are cancelled analytically.

III. WAVES IN THE CHROMOSPHERE AND TRANSITION REGION

Acoustic pulses are seen in the transition region (AFGL-TR-77-0108), but observations of line widths seem to rule out sufficient acoustic flux to heat the upper chromosphere and corona (Athay and White, 1978; Brunner and McWhirter, 1979). Dr. Jorge Vernazza and I have studied the propagation of acoustic waves through the solar atmosphere, and we find that indeed, acoustic waves with velocity amplitudes consistent with the observed wave velocity of $\sim$ 1 km/s at the temperature minimum can not carry sufficient energy to the transition region and the corona to heat them.

We have used a one-dimensional Lagrangian fluid dynamic code, including both electron conduction and optically thin radiative losses (a la Cox and Tucker, 1969) in the energy equation. The waves were driven by a sinusoidal piston in the convection zone, 1.5Mm below $\tau_{5000} = 1$, and propagated through an empirical solar atmospheric model (Vernazza, Averett, Loeser, 1973).

The most surprising result we found was a resonance at 195s period, where the velocity amplitude of the waves at the temperature minimum for a constant driving piston amplitude became very large (Figure 1). This resonance occurs near the acoustic cutoff frequency appropriate to the temperature minimum, but actually seems to have a more global structure and may be the chromospheric mode found by Ando and Osaki (1975). This "200s", "chromospheric" mode extends higher up into the atmosphere than longer period modes and is responsible for the change over in the dominant oscillation frequency from about 300s to about 200s as one goes up in the chromosphere (Figure 2). Both the driving frequency mode and the "200s" mode are excited, but the amplitude of the long period oscillation decreases rapidly with height above $\tau = 1$, while the amplitude of the "200s" mode is nearly constant with height until the top of the chromosphere. Oscillations with periods greater than 200s excite this "chromospheric" mode,

so in the upper chromosphere only this "200s" mode is observed. Oscillations with periods shorter than 200s do not excite the "chromospheric" mode and have large amplitude in the upper chromosphere.

The implications for coronal heating of our results, are that acoustic waves of all periods, 50s $< P <$ 300s with velocity amplitude $\leq$ 1 km/s at the temperature minimum carry $\leq 2 \times 10^4$ ergs/cm^{2}s into the transition region. This is an order of magnitude less than the required energy input into the corona (Figure 3). Even increasing the driving amplitude does not significantly increase the acoustic flux in the transition region. Rather larger driving amplitudes lead to greater wave dissipation in the upper chromosphere (Figure 4).

Hence, on both observational and theoretical grounds acoustic waves are ruled out as the energy supply for the corona. The heating of the upper chromosphere is still an open question. Magnetic fields clearly play a role in the structure of the upper chromosphere. But, the nature of that role is as yet unclear. Magnetic fields may alter the wave generation, they certainly change the types of waves that can propagate and their propagation and dissipation properties, finally the field channels heat conducted back down from the corona to about 20,000K. On the observational side, the large Ca II and Mg II emission is confined to the regions of strong magnetic field in the network. However, Ca II H and K bright points on the blue side of the line are fairly uniformly distributed over the solar disk throughout the interiors of cells, and are likely due to upward propagating acoustic waves. As one step in exploring the effects of magnetic fields we have calculated the shapes of wave-vector surfaces for magneto-acoustic-gravity waves.

IV. MAGNETO-ACOUSTIC-GRAVITY WAVES

The solar corona and chromosphere require some non-thermal energy input to heat them. This energy must be transported by motions: either wave or quasi-static. These motions are produced either directly by the turbulent convective velocity field or by some type of thermal overstability. Typical times scales are comparable to or longer than the natural buoyancy time scale, so that gravity significantly influences the motions. Because the atmosphere is compressible, gas pressure influences the motions as well. We also know that the structure of the corona is controlled by the magnetic field, which must therefore play a crucial role in the process of energy transfer and dissipation. Dissipation likely takes the form of current dissipation in the ionized corona, but the energy that drives these currents must be transferred from the convective zone to the upper atmosphere by wave and quasi-static motions. (Except for currents carried up into the corona by emerging flux, which is a transient phenomena.) Hence the energy transport process will be significantly influenced by three forces: pressure, gravity and magnetic. Nelson Hartunian and I explored some of the propagation properties waves under the influence of these three restoring forces: magneto-acoustic-gravity (M.A.G.) waves. We know that acoustic waves are incapable of supplying sufficient energy to heat the corona. Can the broader class of MAG waves supply all the non-radiative energy input needed to heat the corona?

Before venturing into calculations with the full MAG wave equations, an understanding of the wave properties in the WKB limit is a helpful guide. We have restricted our attention to the case of constant sound speed s and Alfven speed a. This is unrealistic. While an atmosphere can

have constant magnetic field $\underset{\sim}{B}_o$ and temperature T, an atmosphere in hydrostatic equilibrium must have density ρ decreasing outward, so the Alfven speed $a = B_o/(4\pi\rho)^{\frac{1}{2}}$ will increase outward. By neglecting the variation of Alfven speed, we restrict ourselves to the local dispersion relation (McLellan and Winterberg, 1968). This is valid only for wavelengths small compared to the density scale height. On the Sun we are interested in waves with wavelengths comparable to the scale height, so we must integrate the full wave equation. However, the local dispersion relation is already complicated, and a picture of its properties will be a useful guide in the full calculations. The variation in Alfven speed with height was considered by Yeh (1974), but he only examined the special cases of horizontal and vertical magnetic field. The local dispersion relation has been studied for special cases by several authors. Bel and Mein (1971) and Bel and Leroy (1977) have discussed the case of vertical propagation and derived the variation of the acoustic cutoff frequency with magnetic field strength and direction. The special cases of propagation either in or perpendicular to the $\underset{\sim}{g}$-$\underset{\sim}{B}_o$ plane and vertical or horizontal $\underset{\sim}{B}_o$ have been discussed by Chen and Lykoudis (1972, Michalitsanos (1973) and Nakagawa, Priest and Wellck (1973). We consider the general case and study the wave vector surfaces of the local dispersion relation for magneto-acoustic-gravity (MAG) waves to gain insight into the behavior of these waves. The wave vector surface is the three dimensional locus of the real part of the wave vector for all waves at a given frequency. The wavelength is given by $|\mathrm{Re}\ \underset{\sim}{k}| = 2\pi/\lambda$, so, for example, small wave vectors correspond to large wavelengths, and since the phase speed is $c = \omega/|\mathrm{Re}\ \underset{\sim}{k}|$, waves with small wave vectors propagate rapidly. Each type of restoring force tends to give the wave vector surface a distinctive shape as we discuss below. We illustrate and discuss the

wave vector surfaces of MAG waves in general cases in the next section. Analytic results for limiting cases of (i) high frequency, (ii) vertical propagation, (iii) large horizontal wave vector $k_\perp$, and (iv) horizontal magnetic field are derived in an appendix. The principle results are: (1) At high frequencies, where buoyancy is negligible, MAG waves behave like magnetohydrodynamic (MHD) waves. (2) At low frequencies in a weak magnetic field there are both a gravity fast mode and a magnetic slow mode, but these exist only for small wave vectors. At large $|\underset{\sim}{k}|$ both their wave vector surfaces degenerate into planes through the origin in $\underset{\sim}{k}$-space perpendicular to the magnetic field. (3) At low frequencies in a strong magnetic field there is a magnetic pressure fast mode with spheroidal wave vector surface about the origin in k-space. The gravity mode is suppressed except for directions nearly perpendicular to the $\underset{\sim}{B}_o - \underset{\sim}{g}$ plane or for nearly vertical magnetic field. Away from the origin both modes' wave vector surfaces become planes through the origin in $\underset{\sim}{k}$-space perpendicular to the magnetic field. (4) There is a critical frequency separating high from low frequency behavior, which results from the density stratification of the atmosphere. The horizontal component of the magnetic field increases the density scale height and thus reduces the critical frequency.

A. WAVE VECTOR SURFACES

The local dispersion relation for magneto-acoustic-gravity (MAG) wave is

$$\left[\omega^2 - \frac{(\underset{\sim}{k} \cdot \underset{\sim}{B}_o)^2}{4\pi\rho_o}\right]\left[\omega^4 - \omega^2 \left\{(s^2 + a^2)\underset{\sim}{k}^2 - i\gamma \underset{\sim}{g}.\underset{\sim}{k}\right\} + s^2 \underset{\sim}{k}^2 \frac{(\underset{\sim}{k} \cdot \underset{\sim}{B}_o)^2}{4\pi\rho} + (\gamma-1)\, g^2 k_\perp^2 - i\gamma k^2 \frac{(\underset{\sim}{k} \cdot \underset{\sim}{B}_o)(\underset{\sim}{g} \cdot \underset{\sim}{B}_o)}{4\pi\rho_o}\right] = 0 \qquad (1)$$

(McLellan and Winterberg, 1968). Here $\underset{\sim}{B}_o$ is the unperturbed magnetic field, ρ_o is the ambient density, $k_\perp$ is the horizontal component of the wave vector $\underset{\sim}{k}$, $s = (\gamma p_o/\rho_o)^{1/2}$ is the sound speed, $a = \underset{\sim}{B}_o/(4\pi\rho)^{1/2}_o$ is the Alfven speed, and γ is the ratio of specific heats. We solve this for $k\ (\omega, \underset{\sim}{g}, \underset{\sim}{B}_o)$. The first factor is quadratic in k and represents the usual Alfven waves, which we discuss no further. The second factor is quartic in k and represents the MAG waves. In the limit of zero magnetic field it reduces to the dispersion relation for acoustic-gravity waves. In the limit of zero gravity it reduces to the dispersion relation for magneto-hydrodynamic (MHD) waves, and in the limit of zero compressibility (γ, s, $H = p_o/\rho_o g \to \infty$) it reduces to the dispersion relation for magneto-gravity waves.

The wave vector surface is the three-dimensional surface of those values of the real part of the wave vector, Re $\underset{\sim}{k}\ (\omega, \underset{\sim}{g}, \underset{\sim}{B}_o)$, that satisfy the dispersion relation for a given frequency ω. Energy propagates perpendicular to this surface. We will study three-dimensional pictures of the wave vector surface and two-dimensional slices through the surface to help clarify its shape. One can recognize the type of wave mode from the shape of its wave vector surface. Where pressure is the dominant restoring force (acoustic or magnetic pressure modes), there is no preferred direction and the wave vector surface is a spheroid about the origin in $\underset{\sim}{k}$-space.

Where buoyancy is the dominant restoring force the vertical (-g) is the preferred direction. Gravity produces a characteristic acceleration for each direction of fluid displacement. Each direction of motion therefore corresponds to a particular frequency. Because the fluid is not compressed the motion is transverse, $\underset{\sim}{k} \cdot \underset{\sim}{u} = 0$. Since at any given frequency motion is possible only at a single angle to the vertical, the wave vector must make the complementary angle to the vertical and the wave vector surface is a cone of revolution about the vertical axis. Where magnetic tension is the dominant restoring force the magnetic field $\underset{\sim}{B}_o$, is the preferred direction. Magnetic field lines act like rubber bands under tension. Waves are transverse and propagate along the field lines with a characteristic speed equal to the square root of the tension divided by the density. The wave vector surfaces are planes perpendicular to $\underset{\sim}{B}_o$.

The character of the MAG waves depends on their frequency and the magnetic field strength. Frequency is scaled by $N_{ac} = \gamma g/2s$, the acoustic cutoff frequency in the absence of a magnetic field. For high frequencies, $\omega/N_{ac} >> 1$, gravity is unimportant because the fluid acceleration is much larger than g, so the waves behave as fast and slow mode MHD waves (see appendix eqns A4, A5). Acoustic waves cannot propagate at frequencies below the acoustic cutoff frequency. For low frequency waves, $\omega/N_{ac} < 1$, gravity is significant. Magnetic field strength is parametrized by the ratio of Alfven to sound speeds, $a/s = (B_o^2/4\pi\gamma\rho_o)^{\frac{1}{2}} \simeq (P_{mag}/P_{gas})^{\frac{1}{2}}$. For weak fields we expect to find an acoustic-gravity mode plus a slow magnetic mode. For a strong field, we expect to find MHD waves in the high frequency limit and a new situation where all three restoring forces are important in the low frequency limit. We now consider these cases, starting with the simplest situation - high frequencies, where gravity is unimportant. Detailed analytic results are derived, where possible, in the appendix.

1. High Frequency

High frequency means frequency above the acoustic cutoff frequency, where gravity is negligible. In the absence of a magnetic field the acoustic cutoff is

$$N_{ac} = \gamma g/2s = s/2H, \qquad (2)$$

where $H = P_o/\rho_o g$ is the pressure and density scale height. A magnetic field reduces the acoustic cutoff frequency because it increases the scale height. (A cutoff marks a transition between waves that propagate vertically and those that don't, but instead vary exponentially with height.)

Three dimensional pictures of the wave vector surfaces for frequencies above the acoustic cutoff frequency are shown in figures 5 and 6 for the cases of strong and weak magnetic fields respectively. Cuts through the wave vector surfaces at 45^{o} to the $\underline{B}_o$ -g plane are shown in figures 7 and 8. In both cases, as expected, the surfaces look like the usual MHD surfaces because for $\omega \ll N_{ac}$ the effect of gravity is negligible. The spheroidal wave vector surface near the origin is the fast mode and the planar wave vector surfaces on either side of it are the slow mode. In a weak magnetic field: the fast mode is an acoustic mode and has a cutoff frequency, below which it ceases to propagate. The slow mode is a magnetic tension mode and propagates for all frequencies, so it has no cutoff frequency. In a strong magnetic field: the fast mode is a magnetic pressure mode and propagates for all frequencies, so it has no cutoff frequency. The slow mode is a one-dimensional acoustic wave propagating along the magnetic flux tubes and has a cutoff frequency, below which it ceases to propagate.

The acoustic cutoff frequency can be found by considering the special case of vertical propagation (see Appendix and Bel and Mein, 1971; Bell and Leroy, 1977). In the weak field limit, the fast mode has the cutoff frequency (eqn. A12)

$$\omega_{ac} = N_{ac}\, s/(s^2 + a^2\sin^2\theta)^{\frac{1}{2}}, \quad s \gg a. \tag{3a}$$

Below this critical frequency the fast mode becomes an internal gravity mode. In the strong field limit, for a non-horizontal magnetic field, the slow mode has the cutoff frequency (eqn. A20)

$$\omega_{ac} = N_{ac}\cos\theta, \qquad a \gg s, \quad \theta < \pi/2. \tag{3b}$$

Here θ is the polar angle of the magnetic field $\underline{B}_o$. Below this critical frequency the slow mode does not propagate except in a few special directions.

The minimum value of the acoustic mode cutoff frequency for any magnetic field strength occurs for a horizontal magnetic field and is (A22, A43)

$$\omega_{ac} = N_{ac}\, s/(s^2 + a^2)^{\frac{1}{2}}. \tag{3c}$$

These result on the cutoff frequency must be treated with caution, because the WKB approximation is invalid near the cutoff.

The acoustic mode has $\mathrm{Im}\ k_z \simeq -i/2H$ (fig 8b, and eqns. A12, A19, A38), as we would expect from our experience with acoustic-gravity waves. The magnetic mode has $\mathrm{Im}\ k_z \simeq 0$ (fig 8b, and eqns. A14, A16). These are general properties, that are approximately true for all magnetic field strengths. They are a consequence of energy conservation. The wave energy flux,

$$F = \rho u^2 V_{group} \simeq \begin{cases} \rho u^2 s & \text{(acoustic)} \\ \rho u^2 a & \text{(magnetic)}, \end{cases} \tag{4}$$

must be constant with height. For acoustic waves in an isothermal atmosphere, where s = constant,

$$u \propto \rho^{-\frac{1}{2}} \propto e^{-z/2H}. \tag{5}$$

The WKB expression for the velocity amplitude is

$$u \propto |\, \underset{\sim}{k}\, |^{-\frac{1}{2}}\ e^{ik_z z}, \tag{6}$$

and

$$|\, \underset{\sim}{k}\, | \simeq \omega/s = \text{constant}, \tag{7}$$

so

$$\mathrm{Im}\ k_z = -\ 1/2H \quad \text{(acoustic)}. \tag{8}$$

For magnetic waves,

$$a \propto \rho^{-\frac{1}{2}} \propto e^{-\ z/2H}, \tag{9}$$

so

$$u \propto \rho^{-1/4}, \tag{10}$$

but

$$| \underset{\sim}{k} | \approx \omega/a \propto \rho^{\frac{1}{2}}. \tag{11}$$

Hence the height variation of the velocity amplitude of magnetic waves is due to the variation of $| \underset{\sim}{k} |^{-\frac{1}{2}}$ and not the exponential factor, so

$$\mathrm{Im}\, k_z \approx 0 \qquad \text{(magnetic)}. \tag{12}$$

Different modes will couple with each other when their frequencies and wavelengths are the same. For large $| \underset{\sim}{k} |$ there is at most one upward and downward propagating wave, so no coupling can occur, but for small $| \underset{\sim}{k} |$ coupling is sometimes possible. The magnetic and acoustic modes will have intersecting wave vector surfaces when $a > s$. Consider the limiting case of vertically propagating waves. The coupling condition can be found by equating the expressions for the real parts of the fast and slow wave vector (eqns. A10 and A19), and solving for ω. Resonant coupling occurs, when $a \gg s$, for

$$\omega/N_{ac} = \cos\theta \left(1 + s^2 \cos^2\theta/a^2\right)^{\frac{1}{2}},$$

$$\mathrm{Re}\, k_z = \frac{\cos\theta}{2H} \frac{s}{a}, \tag{13}$$

that is for ω slightly above the cutoff frequency and wavelength larger than the scale height. Bel and Leroy (1977) have obtained corresponding results for a vertical field of arbitrary strength.

2. Low Frequency

We now turn our attention to the more interesting but complicated case of low frequencies where all three forces are significant.

(a) Weak Magnetic Field

In a weak magnetic field one mode must be a gravity wave and the other a slow mode magnetic tension wave, in order to go continuously to the limit of acoustic-gravity waves in the absence of a magnetic field and MHD waves in the absence of gravity. This is indeed the case, as shown in the three-dimensional wave vector surface pictures (fig. 9) and slices through the wave vector surface in figure 10. There are some modifications, however. First, the gravity mode hyperbola is cut off near the Alfven planes. This is similar to the wave vector surfaces of magneto-gravity waves (Lighthill, 1967; Schwartz and Stein, 1975). Second, the slow mode wave vector surface has a bulge away from the origin in the vertical direction, rather than a dimple toward the origin in the magnetic field direction as found in MHD waves. Third, at large horizontal wave vector, $k_\perp >> \omega/\min$ (s, a), both modes wave vector surfaces become planes perpendicular to the magnetic field direction whose extensions pass through the origin. This can be seen most easily from the analytic results derived in the appendix (eqn. A40) and from slices through the wave vector surface when the magnetic field is nearly vertical (fig. 11). When a wave vector surface becomes a plane through the origin perpendicular to the magnetic field, its group velocity goes to infinity, since $\underset{\sim}{k}$ is independent of ω, and its potential energy becomes much larger than its kinetic energy. This occurs below the critical frequency

$$\omega_c = N\cos\theta \qquad (14)$$

(A36, where $N = (\gamma-1)^{\frac{1}{2}} g/s$ is the Brunt Väisälä frequency) for both the fast gravity and slow magnetic modes at sufficiently large $|\underset{\sim}{k}|$. The propagation direction perpendicular to the $\underset{\sim}{B}_o - \underset{\sim}{g}$ plane is a special case. In this direction the plane through the origin in $\underset{\sim}{k}$ - space perpendicular to the magnetic field has zero vertical component. Hence in this direction at large $k_\perp$ the wave vector surfaces arch over until Re $k_z = 0$ (fig 12). In this special case there is a sharp cutoff to propagation. However, in general whenever the wave vector surface approaches a plane through the origin perpendicular to the magnetic field (Re $\delta \to o$ in A31) the waves become non-propagating.

(b) Strong Magnetic Field

As the magnetic field strength increases, the distance of the Alfven planes from the origin, ω/a, decreases. Any gravity mode wave vector surface is restricted to lie between these planes, on which magnetic tension provides all the needed acceleration. Hence the gravity mode wave vector surface gets squashed (figs 13-15). Instead of a hyperboloid, the wave vector surface degenerates into two intersecting planes through the origin - one perpendicular to the magnetic field and the other with $k_z = 0$. The critical frequency for both zero and large $k_\perp$ is the same in the strong field limit (eqns. A20 and A35)

$$\omega_c = N_{BV} \cos\theta . \qquad (15)$$

Hence a gravity wave slow mode cannot propagate in a strong magnetic field, except for a small range of intermediate $k_\perp$ and directions nearly perpendicular the $\underset{\sim}{B}_o$ - $\underset{\sim}{g}$ plane (fig 16) or nearly vertical magnetic field (fig 17). These last two figures also clearly illustrate the degeneration of the wave vector surfaces at large $k_\perp$ into planes through the origin perpendicular to the magnetic field. Again Re $k_z = 0$ on this plane in the special direction perpendicular to the $\underset{\sim}{B}_o$ - $\underset{\sim}{g}$ plane.

The wave vector surface of the second mode - the magnetic pressure fast mode - remains a spheroid about the origin at low frequency (figs 13-15) as at high frequency (fig 5). However, at low frequency this spheroid attaches onto a plane through the origin perpendicular to the magnetic field at large $k_\perp$, rather than terminating as at high frequencies. These waves with large $k_\perp$ have virtually all their energy in the form of magnetic potential energy.

(c) Conclusion

The significance of these results for solar heating are: First, all low frequency waves ($\omega < N\cos\theta$) in a strong magnetic field propagate energy in the direction of the magnetic field. Thus refraction will not reduce the energy flux of low frequency waves. Second, the group velocity of such waves may be greater than the Alfven speed. And third, the magnetic energy density will be greater than the kinetic energy density. Because of these last two results, the total wave flux will not be observable in line widths or Doppler shifts. Hence current observations do not place any restrictions on the flux of low frequency M.A.G. waves.

Appendix: Limiting Cases

The local dispersion relation for magneto-acoustic-gravity waves (neglecting gradients in the sound and Alfven speeds) is (McLellan and Winterberg, 1968)

$$\omega^4 - \omega^2 \left[(s^2 + a^2)\, \underset{\sim}{k}^2 - i\gamma \underset{\sim}{g} \cdot \underset{\sim}{k} \right] + \left[s^2 \underset{\sim}{k}^2 \frac{(\underset{\sim}{k} \cdot \underset{\sim}{B}_o)^2}{4\pi\rho_o} + (\gamma-1)\, \underset{\sim}{g}^2 k_\perp^2 - i\gamma \underset{\sim}{k}^2 \frac{(\underset{\sim}{k} \cdot \underset{\sim}{B}_o)(\underset{\sim}{g} \cdot \underset{\sim}{B}_o)}{4\pi\rho_o} \right] = 0, \tag{A1}$$

where $\underset{\sim}{B}_o$ is the ambient magnetic field, ρ_o is the ambient density, $k_\perp$ is the horizontal component of the wave vector $\underset{\sim}{k}$, and γ is the ratio of specific heats. This dispersion relation is a fourth order equation for the complex vertical component k_z of the wave vector in terms of the frequency and horizontal component $k_\perp$, which are real:

$$D = a k_z^4 + b k_z^3 + c k_z^2 + d k_z + e = 0 \tag{A2}$$

where

$$a = s^2 a^2 \cos^2\theta$$

$$b = 2 s^2 a^2 k_\perp \cos\theta \sin\theta \cos\phi + i\gamma g a^2 \cos^2\theta$$

$$c = -\omega^2 (s^2 + a^2) + s^2 a^2 k_\perp^2 (\cos^2\theta + \sin^2\theta \cos^2\phi) + i\gamma g a^2 k_\perp \cos\theta \sin\theta \cos\phi$$

$$d = 2 s^2 a^2 k_\perp^3 \cos\theta \sin\theta \cos\phi - i\gamma g \omega^2 + i\gamma g a^2 k_\perp^2 \cos^2\theta$$

$$e = \omega^4 - \omega^2 (s^2 + a^2) k_\perp^2 + s^2 a^2 k_\perp^4 \sin^2\theta \cos^2\phi + (\gamma - 1) g^2 k_\perp^2 + i\gamma g a^2 k_\perp^3 \cos\theta \sin\cos\phi. \tag{A3}$$

θ is the polar angle between the magnetic field and the vertical and ϕ is the azimuthal angle between the horizontal projections of the magnetic field and the wave vector-vertical plane.

(i) High Frequency

For high frequencies, $\omega >> g/s$, gravity is negligible and the M.A.G. waves become the well known MHD waves. The dispersion relation reduces to

$$\omega^4 - \omega^2 (s^2 + a^2) \underset{\sim}{k}^2 + s^2 \underset{\sim}{k}^2 \frac{(\underset{\sim}{k}.\underset{\sim}{B}_o)^2}{4\pi\rho_o} = 0 \qquad \text{(A4)}$$

or

$$c^4 - c^2 (s^2 + a^2) + s^2 a^2 \cos^2 \theta_{kB} = 0$$

where $c = \omega/k$ is the wave's phase velocity and θ_{kB} is the angle between k and $\underset{\sim}{B}_o$. The wave modes in this case are the usual fast and slow modes. Their phase velocity is

$$c_{\pm}^2 = \frac{s^2 + a^2}{2} \pm \tfrac{1}{2} \left[(s^2 + a^2)^2 - 4 s^2 a^2 \cos^2 \theta_{kB} \right]^{\frac{1}{2}} \qquad \text{(A5)}$$

In the limits a>>s or s>>a, the phase velocities are

$$c_{fast}^2 = c_>^2 + c_<^2 \sin^2 \theta_{kB}$$

$$c_{slow}^2 = c_<^2 \cos^2 \theta_{kB} \qquad \text{(A6)}$$

where $c_> = \max(s, a)$ and $c_< = \min(s, a)$ (see for instance Bazer and Fleischman, 1959.) In the weak field limit the fast mode is an acoustic mode and the slow mode a magnetic tension mode, while in the strong field limit the fast mode is a magnetic pressure mode and the slow mode a one dimensional acoustic mode propagating along the magnetic flux tubes.

(ii) Vertical Propagation

For vertical propagation, $k_\perp = 0$, the dispersion relation reduces to (Bell and Mein, 1971)

$$\left(\frac{\omega}{k}\right)^4 - \left(\frac{\omega}{k}\right)^2 \left[a^2 + s^2 \left(1 + \frac{i}{kH}\right) \right] + a^2 s^2 \left(1 + \frac{i}{kH}\right) \cos^2 \theta = 0 \qquad \text{(A7)}$$

where $H = P/\rho g = s^2/\gamma g$ is the pressure scale height in an isothermal atmosphere. This is similar to the MHD dispersion relation, with $s^2 \to s^2\,(1 + i/kH)$. The phase velocities are now a function of k

$$c_{\pm}^2 = \frac{a^2 + s^2(1 + i/kH)}{2} \pm \tfrac{1}{2}\left[(a^2 + s^2)^2 - \left(\frac{s^2}{kH}\right)^2 + 2i\,\frac{s^2}{kH}\,(s^2 + a^2) - 4\,(1 + \frac{i}{kH})\,s^2a^2\cos^2\theta\right]^{\frac{1}{2}} \qquad \text{(A8)}$$

In the weak and strong field limits this becomes

$$c_{fast}^2 = \left(\frac{\omega}{k}\right)_+^2 = s^2\,(1 + \frac{i}{kH}) + a^2\sin^2\theta \qquad s>>a \qquad \text{(A9)}$$

$$= a^2 + s^2\,(1 + \frac{i}{kH})\,\sin^2\theta \qquad a>>s$$

$$c_{slow}^2 = \left(\frac{\omega}{k}\right)_-^2 = \frac{a^2s^2(1 + i/kH)\cos^2\theta}{a^2 + s^2\,(1 + i/kH)} \qquad \text{(A10)}$$

$$= a^2\cos^2\theta \qquad s>>a$$

$$= s^2\,(1 + \frac{i}{kH})\,\cos^2\theta \qquad a>>s$$

These can be solved for the wave vector k. Consider four cases separately.

(a) Fast mode with s>>a:

$$k^2\,(s^2 + a^2\sin^2\theta) + i(k/H)\,s^2 - \omega^2 = 0\,, \qquad \text{(A11)}$$

so

$$k_+ = -\frac{i}{2H}\,\frac{s^2}{s^2 + a^2\sin^2\theta} \pm \sqrt{\frac{\omega}{s^2+a^2\sin^2\theta}}\left[1 - \frac{N_{ac}^2}{\omega^2}\,\frac{s^2}{s^2+a^2\sin^2\theta}\right]^{\frac{1}{2}}, \qquad \text{(A12)}$$

where $N_{ac} = \gamma g/2s = s/2H$.

There is a cutoff frequency, below which the wave is evanescent,

$$\omega_{crit} = N_{ac} \; s/\left[s^2 + a^2\sin^2\theta\right]^{1/2}. \tag{A13}$$

This mode is a cross between the acoustic branch of acoustic-gravity waves and the fast mode MHD wave. The stratification produces the cutoff frequency and a vertical amplitude growth (imaginary part of the wave vector). The magnetic field reduces the cutoff frequency below N_{ac} and reduces the vertical growth rate below 1/2H, their values for acoustic-gravity waves.

(b) Slow mode with s>>a

$$k_z = \pm \frac{\omega}{a\cos\theta} \tag{A14}$$

This is the usual magnetic tension slow mode. Gravity does not alter the mode.

(c) Fast mode with a>>s

In the case where $kH>>s^2/a^2$

$$k^2(a^2 + s^2\sin^2\theta) + i(k/H)\, s^2\sin^2\theta - \omega^2 = 0 \tag{A15}$$

so

$$k_z = -\frac{i}{2H}\,\frac{s^2\sin^2\theta}{a^2} \pm \frac{\omega}{\sqrt{a^2+s^2\sin^2\theta}}\left[1 - \frac{N_{ac}^2}{\omega^2}\,\frac{s^2\sin^2\theta}{a^2}\right]^{1/2} \tag{A16}$$

This is a magnetic pressure mode slightly modified by gravity. There is a small vertical growth in amplitude and a slight dependence of the phase velocity on the direction of the magnetic field. There is no cutoff frequency contrary to appearances, because as $\omega \to N_{ac}\left(\frac{s}{a}\right)$, $kH \to s^2/a^2$ and our initial assumption is no longer valid. The case of small kH must be investigated separately.

The special case $kH < s^2/a^2$ corresponds to small frequencies, $\omega/N_{ac} < s/a$. In this case the vertical dispersion relation reduces to

$$\left(\frac{\omega}{k}\right)^3 - i\left(\frac{\omega}{k}\right)\frac{s^2}{kH} + i\,\frac{s^2a^2\cos^2\theta}{\omega H} = 0,$$

which can be written as a cubic equation for the wave vector

$$k^3 - k\,\frac{\omega^2}{a^2\cos^2\theta} - i\,\frac{\omega^4 H}{a^2 s^2\cos^2\theta} = 0\,. \qquad \text{(A17)}$$

In the limit of small ω, the first and second terms dominate, and

$$k = \pm\,\frac{\omega}{a\cos\theta}\,.$$

If we include the first order correction, we find that the fast mode at very low frequency in the strong field case is

$$k_+ = \pm\,\frac{\omega}{a\cos\theta} + \frac{i}{8H}\left(\frac{\omega}{N_{ac}}\right)^2\,. \qquad \text{(A18)}$$

The third root of the cubic is pure imaginary. This is a magnetic tension mode and has no cutoff frequency.

(d) Slow mode with a>>s:

$$k^2s^2\cos^2\theta + i\,(k/H)\,s^2\cos^2\theta - \omega^2 = 0\,,$$

so

$$k_- = -\,\frac{i}{2H} \pm \frac{\omega}{s\cos\theta}\left[1 - \frac{N_{ac}^2\cos^2\theta}{\omega^2}\right]^{1/2}\,. \qquad \text{(A19)}$$

This is an acoustic mode. Its phase velocity in the direction of B_o is the sound speed. It grows in the vertical direction with the usual scale height of 2H. It has a cutoff frequency

$$\omega_{crit} = N_{ac}\cos\theta. \qquad \text{(A20)}$$

The case of a horizontal field must be treated separately. For $\theta = 90^{o}$ one mode has zero phase velocity and the dispersion relation for the other mode becomes

$$\omega^2 - (a^2 + s^2)\, k^2 - \frac{ik}{H}\, s^2 = 0 \ ,$$

so

$$k = -\frac{i}{2H}\,\frac{s^2}{a^2 + s^2} \pm \sqrt{\frac{\omega}{a^2 + s^2}}\left[1 - \frac{N_{ac}^{\ 2}}{\omega^2}\,\frac{s^2}{a^2 + s^2}\right]^{\frac{1}{2}} . \qquad \text{(A21)}$$

In this case the cutoff frequency is

$$\omega_{crit} = N_{ac}\left[\frac{s^2}{a^2 + s^2}\right]^{\frac{1}{2}} \qquad \text{(A22)}$$

and the vertical growth rate is reduced.

(iii) Large $k_\perp$

In the limit of large $k_\perp$, that is $k_\perp >> \omega/\min(a,s)$ the dominant terms in the dispersion relation are the terms of order k^4:

$$k_z^{\ 4}\ a^2 s^2 \cos^2\theta + 2k_z^{\ 3}\, k_\perp a^2 s^2 \cos\theta\sin\theta\cos\phi$$

$$+ k_z^{\ 2}\, k_\perp^{\ 2}\, a^2 s^2\, (\cos^2\theta + \sin^2\theta\cos^2\phi)$$

$$+ 2k_z\, k_\perp^{\ 3}\, a^2 s^2\, \cos\theta\sin\theta\cos\phi$$

$$= (k_z^{\ 2} + k_\perp^{\ 2})\ \ (k_z\cos\theta + k_\perp\sin\theta\cos\phi)^2\, a^2 s^2$$

$$= s^2\, \underset{\sim}{k}^2\, \frac{(\underset{\sim}{k} \cdot \underset{\sim}{B}_o)^2}{4\pi\rho_o}$$

$$= 0. \qquad \text{(A23)}$$

Hence either

$$\underset{\sim}{k} \cdot \underset{\sim}{B}_o \to 0, \tag{A24}$$

or

$$\underset{\sim}{k}^2 = 0, \quad \text{i.e.} \quad k_z^2 = - k_\perp^2. \tag{A25}$$

The next lower terms are the terms of order k^3, and the dispersion relation is

$$\underset{\sim}{k}^2 \frac{(\underset{\sim}{k} \cdot \underset{\sim}{B}_o)^2}{4\pi\rho_o} - i\gamma \underset{\sim}{k}^2 \frac{(\underset{\sim}{k} \cdot \underset{\sim}{B}_o)(\underset{\sim}{g} \cdot \underset{\sim}{B}_o)}{4\pi\rho_o s^2}$$

$$= \underset{\sim}{k}^2 \frac{\underset{\sim}{k} \cdot \underset{\sim}{B}_o}{4\pi\rho_o} \left[\underset{\sim}{k} \cdot \underset{\sim}{B}_o - i\gamma \underset{\sim}{g} \cdot \underset{\sim}{B}_o / s^2 \right]$$

$$= (k_z^2 + k_\perp^2) \quad (k_z \cos\theta + k_\perp \sin\theta\cos\phi)$$

$$\left[k_z \cos\theta + k \sin\theta\cos\phi + i\cos\theta/H \right] a^2$$

$$= 0 . \tag{A26}$$

The four roots are

(1) $\underset{\sim}{k} \cdot \underset{\sim}{B}_o = 0$

or

$$k_z = - k_\perp \tan\theta\cos\phi \tag{A27}$$

(2) $\underset{\sim}{k} \cdot \underset{\sim}{B}_o = i\gamma \underset{\sim}{g} \cdot \underset{\sim}{B}_o / s^2$

or

$$k_z = - k_\perp \tan\theta\cos\phi - i/H \tag{A28}$$

(3 and 4) $\underset{\sim}{k}^2 = 0$

or

$$k_z = \pm i k_\perp \tag{A29}$$

The first two modes have wave vector surfaces that are planes perpandicular to $\underset{\sim}{B}_o$, while the last two are non-propagating modes. For the first two modes we can include the next lower order, $\underset{\sim}{k}^2$, terms in the dispersion relation as a perturbation. The dispersion relation now becomes

$$\underset{\sim}{k}^2 \quad \frac{\underset{\sim}{k} \cdot \underset{\sim}{B}_o}{4\pi\rho_o} \left[\underset{\sim}{k} \cdot \underset{\sim}{B}_o - i\gamma \underset{\sim}{g} \cdot \underset{\sim}{B}_o / s^2 \right]$$

$$+ N^2 k_\perp^2 - \underset{\sim}{k}^2 \quad \frac{s^2 + a^2}{s^2} \quad \omega^2 = 0,$$

where $N = (\gamma - 1)^{\frac{1}{2}} g/s$ is the Brunt-Väisälä the frequency of oscillation of a fluid parcel in an isothermal atmosphere.
In component form

$$(k_z^2 + k_\perp^2) \quad (k_z \cos\theta + k_\perp \sin\theta\cos\phi)$$

$$x \left[k_z \cos\theta + k_\perp \sin\theta\cos\phi + i\cos\theta/H \right]$$

$$- (k_z^2 + k_\perp^2) \quad \frac{s^2 + a^2}{s^2 a^2} \quad \omega^2 + \frac{N^2}{a^2} \quad k_\perp^2 = 0. \tag{A30}$$

Let us define δ by

$$k_z = - \quad k_\perp \tan\theta\cos\phi + \delta. \tag{A31}$$

then

$$k_z \cos\theta + k_\perp \sin\theta\cos\phi = \delta\cos\theta \tag{A32}$$

and

$$k_z^2 + k_\perp^2 = \quad k_\perp^2 \left(\tan^2\theta\cos^2\phi + 1\right) - 2\delta k_\perp \tan\theta\cos\phi.$$

The dispersion relation becomes (note $\delta \sim H^{-1}$)

$$\delta \cos^2\theta \quad (\delta + i/H) - \omega^2 \quad (a^2 + s^2) \, / a^2 s^2$$

$$+ (N^2/a^2) \, / \, (\tan^2\theta\cos^2\phi + 1) = 0.$$

Hence

$$\delta = -\frac{i}{2H} \pm \left[\frac{\omega^2}{\cos^2\theta} \frac{s^2 + a^2}{a^2 s^2} - \frac{1}{4H^2} - \frac{N^2}{a^2} \frac{1}{1 - \sin^2\theta \sin^2\phi} \right]^{\frac{1}{2}}, \tag{A33}$$

There exists a critical frequency

$$\omega_c^2 = \frac{a^2 s^2}{a^2 + s^2} \left[\frac{\cos^2\theta}{4H^2} + \frac{N^2}{a^2} \frac{1}{1 + \tan^2\theta \cos^2\phi} \right]$$

$$> \frac{a^2 s^2}{a^2 + s^2} \left[\frac{1}{4H^2} + \frac{N^2}{a^2} \right] \cos^2\theta . \tag{A34}$$

The wave vector has a real part, $\delta\cos\theta$, parallel to the magnetic field for $\omega > \omega_c$. However, for $\omega < \omega_c$, $\mathrm{Re}\,\delta = 0$ so the real part of the wave vector is perpendicular to the magnetic field through the origin.

$$\omega_c^2 = N_{ac}^2 \cos^2\theta, \quad (a >> s, \text{ independent of } \phi). \tag{A35}$$

Note this is the same as the cutoff frequency (A20) of the slow acoustic mode in the opposite limit, $k_\perp \to 0$.

For a weak field,

$$\omega_c^2 = N^2 / (1 + \tan^2\theta \cos^2\phi) \qquad (s >> a)$$

$$> N^2 \cos^2\theta . \tag{A36}$$

In this case δ has a real part for all ϕ if $\omega > N$, but only for ϕ inside a fan

$$\cos^2\phi > \left(\frac{N^2}{\omega^2} - 1 \right) / \tan^2\theta \tag{A37}$$

if $N > \omega > N\cos\theta$.

Above the critical frequency
(for high frequencies or nearly horizontal $\underset{\sim}{B}_o$, $\cos\theta \simeq o$)

$$\delta = -\frac{i}{2H} \pm \frac{\omega}{\cos\theta}\sqrt{\frac{s^2 + a^2}{s^2 a^2}} \tag{A38}$$

$$\cdot - \frac{i}{2H} \pm \begin{cases} \dfrac{\omega}{a\cos\theta} & s>>a \\ \dfrac{\omega}{s\cos\theta} & a>>s \end{cases}$$

These are the usual MHD slow modes, but with the usual acoustic-gravity exponential growth factor.

Below the critical frequency ($\omega << \omega_c$), with a>>s

$$\delta = \begin{cases} -i/H \\ +i/H \end{cases} \quad \frac{s^2}{a^2} \quad \frac{\gamma-1}{\gamma^2} \quad \frac{1}{1 - \sin^2\theta\sin^2\phi} \simeq 0 \tag{A39}$$

Hence the wave-vector surfaces are planes through the origin and perpendicular to $\underset{\sim}{B}_o$

Below the critical frequency ($\omega << \omega_c$) with s>>a

$$\delta = \pm i \frac{N}{a} \frac{1}{(1 - \sin^2\theta\sin^2\phi)^{1/2}} - \frac{i}{2H}, \tag{A40}$$

where

$$\frac{N}{a} = \frac{1}{H}\frac{s}{a}\frac{\gamma-1}{\gamma^2}$$

Again the wave-vector surfaces are planes through the origin perpendicular to $\underset{\sim}{B}_o$.

(iv) Horizontal Magnetic Field

When the magnetic field is horizontal, the dispersion relation reduces to a quadratic in k_z (since $\cos\theta = 0$)

$$\omega^4 - \omega^2 \left[(s^2 + a^2) \quad \underset{\sim}{k}^2 - i\gamma \underset{\sim}{g}.\underset{\sim}{k}\right]$$

$$+ \quad (N^2 + a^2 \underset{\sim}{k}^2)\, s^2 k_\perp^2$$

$$= \left[- \omega^2 (s^2 + a^2) + s^2 a^2 k_\perp^2 \cos^2\phi \right] \quad k_z^2$$

$$- i\gamma g\, \omega^2\, k_z$$

$$+ \left[\omega^4 - \omega^2 (s^2 + a^2) k_\perp^2 + s^2 a^2\, k_\perp^4 + N^2 s^2 k_\perp^2\right]$$

$$= 0 \qquad \text{(A41)}$$

For small $k_\perp$ and for all $k_\perp$ at high frequencies this reduces to the usual acoustic - gravity dispersion relation, but with $s^2 \to s^2 + a^2$:

$$\omega^2 (s^2 + a^2)\, k_z^2 + i\gamma g \omega^2\, k_z$$

$$- \left[\omega^4 - \omega^2 (s^2 + a^2) k_\perp^2 + N^2 s^2 k_\perp^2\right] = 0$$

The vertical component of the wave vector is

$$k_z = - \frac{i}{2H} \left(\frac{s^2}{s^2+a^2}\right) \pm \left[\frac{\omega^2}{s^2+a^2} - \frac{1}{4H^2} \left(\frac{s^2}{s^2+a^2}\right)^2 \right.$$

$$\left. + \left(\frac{N^2}{\omega^2} \quad \frac{s^2}{s^2+a^2} \quad -1\right) k_\perp^2 \right]^{\frac{1}{2}}$$

(A42)

There are acoustic or magnetic pressure waves in the high frequency limit and a modified gravity wave in the low frequency limit. The critical frequencies are

$$\omega = \left\{ \begin{matrix} N_{ac} \\ N \end{matrix} \right\} \times \left(\frac{s^2}{s^2+a^2} \right)^{\frac{1}{2}} \tag{A43}$$

so both are reduced by the magnetic field.

For larger $k_\perp$ and low frequencies the dispersion reduces to

$$- \omega^2 (s^2 + a^2) \underset{\sim}{k}^2 + \underset{\sim}{k}^2 s^2 a^2 k_\perp^2 + N^2 s^2 k_\perp^2 = 0.$$

This is the same as the magneto-gravity dispersion relation (for horizontal $\underset{\sim}{B}_o$)

$$- \omega^2 \underset{\sim}{k}^2 + \underset{\sim}{k}^2 a^2 k_\perp^2 + N^2 k_\perp^2 = 0,$$

but with

$$\omega^2 \to \omega^2 \frac{s^2 + a^2}{s^2} .$$

Compare fig. 14 with Schwartz and Stein (1975) fig 3b.

The vertical component of the wave-vector is

$$k_z^2 = \left[\frac{N^2 \frac{s^2}{s^2+a^2}}{\omega^2 - k_\perp^2 \frac{s^2 a^2}{s^2+a^2}} - 1 \right] k_\perp^2 \tag{A44}$$

Hence $k_z \to \infty$ for $k_\perp = \omega^2 \frac{s^2+a^2}{s^2 a^2}$ and is real for smaller $k_\perp$ and ω below the critical frequency.

V. "MODAL" CODE

We wish to study the generation, propagation, and dissipation of magneto-acoustic-gravity waves in order to determine their role in chromospheric and coronal heating, as well as to determine any possible signatures of different waves on line profiles. These waves are inherently three-dimensional and three-dimensional nonlinear MHD calculations require large amounts of computer time. We are therefore developing a method of reducing the three-dimensional calculations to one dimension. The essence of this "modal" method is to assume that the mean state of the atmosphere is horizontally uniform then separate all the fluid variables into mean and fluctuating parts, and expand the fluctuating parts in a complete set of horizontal planforms. The crucial approximation is to truncate this expansion at only a single hexagonal horizontal planform, which then leaves us with a system on one-dimensional Eulerian partial-differential equations for the mean variables and the amplitude of the fluctuating variables. For example, scaler variables are expanded like the density

$$\rho(\underset{\sim}{r},t) = \overline{\rho}\,(z,t) + R\,(z,t)\,f\,(x,y)$$

where $\overline{\rho}$ is the mean and Rf the fluctuating part of the density and f is the hexagonal planform

$$f(x,y) = \frac{1}{\sqrt{6}} \sum_{i=1}^{6} e^{i\underset{\sim}{k}_i \cdot \underset{\sim}{x}}$$

$$\{\underset{\sim}{k}_i\} = \pm\ (0, \frac{4\pi}{3S}),\ \pm\ (\frac{2\pi}{\sqrt{3}S}, \frac{2\pi}{3S}),\ \pm\ (\frac{2\pi}{\sqrt{3}S}, \frac{2\pi}{3S}),$$

where S is the length of a side of the hexagon.

Vector variables are expanded like the velocity in terms of scaler potentials,

$$V(r,t) = \bar{V}(Z,t) + \begin{pmatrix} a^{-1}\{f_x(x,y)\ U\ (z,t) + f_y(x,y)\ \xi\ (z,t)\} \\ a^{-1}\{f_y(x,y)\ U\ (z,t) - f_x(x,y)\ \xi\ (z,t)\} \\ \\ f(x,y)\ W(z,t) \end{pmatrix}$$

These hexagonal horizontal plan forms are shown in Figure 19. We have imposed this fixed horizontal structure on the fluid flow. These 1-mode expansions are substituted in the equations of motion, which are separated into horizontally averaged and fluctuating parts. For example, the continuity equation becomes

$$\frac{\partial \overline{\rho}}{\partial t} + \nabla \cdot (\overline{\rho}\ \underset{\sim}{\overline{v}}) + \frac{\partial}{\partial z}(RW) = 0$$

$$\frac{\partial R}{\partial t} + \frac{\partial}{\partial z}(\overline{\rho}\ W + CRW) = a\,(\overline{\rho}\ U + C^1 RU)$$

where

$$C = \overline{fff} = 2/\sqrt{6}$$

$$C^1 = a^{-2}\ f\ [f_x f_x + f_y f_y] = \frac{C}{2} = {}^1/\sqrt{6}$$

The advantage of this method is that we have included the horizontal velocities and a crude representation of the horizontal variation of the motion, while retaining some of the non-linear coupling because we use hexagonal planforms, and still have only a one dimensional system of equations. The disadvantage is that the horizontal strucutre is imposed and does not correspond to the actual fluid flow. It can, however, be throught of as a standing wave pattern produced by six waves propagating in an hexagonal "pattern".

The modal equations are solved by dividing the atmosphere into a grid of layers and transforming the partial differential equations to finite difference equations on the spatial grid. We solve the finite difference equations using a two step Lax-Wendroff method (Richtmyer and Morton, 1969) with "Flux Corrected

Transport" to introduce additional dissipation to stabilize the scheme (Book, Boris, Hain, 1975). We use the full one-dimensional non-linear Eulerian equations to test the solution scheme. At the moment there is a problem with the FCT scheme at the boundary in a stratified atmosphere. We have tested the modal scheme for (a) one-dimensional piston driven shocks. These show the correct steepening and shock formation, but a bad post shock profile with a kink in the saw tooth profile. (b) We are now calculating waves in an isothermal gas, so only the continuity and momentum equations need to be solved, in order to try and isolate the problem.

REFERENCES

Ando, H. and Osaki, Y. (1975) Publ. Astron. Soc. Japan 27, 581.

Athay, R.G. and White, O.R. (1978) Astrophys. J. 226, 1135.

Bel, N. and Leroy, B. (1977) Astron. and Astrophys. 55, 239.

Bel, N. and Mein, P. (1971) Astron. and Astrophys. 11, 234.

Book, D.L., Boris, J.P. and Hain, K. (1975) J. Comp. Phys. 18, 248.

Brunner, E.C. and McWhirter, R.W.P. (1979) Astrophys. J. 231, 557.

Chen, C.J. and Lykoudis, P. (1972) Solar Phys. 25, 380.

Cox, D.P. and Tucker, W.H. (1969) Astrophys. J. 157, 1157.

Lighthill, M.J. (1967) Aerodynamic Phenomena in Stellar Atmospheres, ed. R. Thomas, IAU Symposium 28.

McLellan, A. and Winterberg, F. (1968) Solar Phys. 4, 401.

Michalitsanos, A. (1973) Solar Phys. 30, 47.

Nakagawa, Y., Priest, E., and Wellck, R. (1973) Astrophys. J. 184, 931.

Richtmeyer, R.D. and Morton, K.W. (1967) "Difference Methods for Initial Value Problems", Interscience, N.Y.

Schwartz, R.A. and Stein, R.F. (1975) Astrophys. J. 200, 499.

Vernazza, J.E., Avrett, E.M. and Loeser, R. (1973) Astrophys. J. 184, 605.

Yeh, T. (1974) Phys. Fluids 17, 2282.

FIGURE CAPTIONS

Fig. 1 Chromospheric Resonance: Velocity Amplitude at the temperature minimum for a given driving piston amplitude, $V_p = 3 \times 10^{-3}$ x sound speed, as a function of driving piston period.

Fig. 2 Modes: Kinetic energy density in the fundamental and harmonic modes as a function of height.

Fig. 3 Transition region flux as a function of driving piston period for a given driving piston amplitude, $V_p = 3 \times 10^{-3}$ x sound speed.

Fig. 4 Transition region flux as a function of driving piston amplitude for driving piston periods of 150 and 300 seconds.

Fig. 5 Wave vector surface at high frequency, $f = \omega/N_{ac} = 1.1$, in a strong magnetic field, $a/s = 3.16$. The axes are k_x, k_y, k_z and full scale along each axis is $\pm 0.75/H$, where H is the pressure and density scale height. The magnetic field lies in the plane of the paper at an angle $\theta = 30^{\circ}$ to the vertical in this and all subsequent 3-dimensional pictures of the wave vector surface, except figure 14. The spheroid in the center is the magnetic pressure fast mode an the planes are the acoustic slow mode propagating along the magnetic flux tubes.

Fig. 6 Wave vector surface at high frequency, $f = \omega/N_{ac} = 1.1$, in a weak magnetic field, $a/s = 0.707$. Full scale along each axis is $\pm$ 1.5/H. The spheroid in the center is the acoustic fast mode and the planes are the magnetic tension slow mode.

Fig. 7 Slice through the wave vector surface at high frequency, $f = \omega/N_{ac} = 1.0$, in a strong magnetic field. The axis are the real part of the vertical, Re k_z, and the horizontal, k_H, components of the wave vector in units of the reciprocal of the scale height, H^{-1}. The magnetic field direction is $\theta = 45^{\circ}$ to the vertical and $\phi = 45^{\circ}$ to the plane of the paper.

Fig. 8 (a) Slice through the wave vector surface at high frequency, $f = \omega/N_{ac} = 1.0$, in a weak magnetic field.

(b) Imaginary part of the vertical component of the wave vector, $\mathrm{Im}\, k_z$, along the same slice as Fig. 4a. Units are H^{-1}.

Fig. 9 (a) Wave vector surface of the gravity fast mode at low frequency, $f = \omega/N_{ac} = 0.5$, in a weak magnetic field.

(b) Wave vector surface of the magnetic tension slow mode. In both cases full scale along each axis is $\pm$ 2/H.

Fig. 10 (a) Slice through wave vector surface at low frequency, $f = \omega/N_{ac} = 0.5$, in a weak magnetic field.

(b) Imaginary part of k_z along the same slice. Units are H^{-1}. θ and ϕ give the direction of B_o.

Fig. 11 (a) Slice through wave vector surface at low frequency, $f = \omega/N_{ac} = 0.5$, in a nearly vertical, $\theta = 5^o$, magnetic field.

(b) Imaginary part of k_z along the same slice. Units are H^{-1}.

Fig. 12 (a) Slice through wave vector surface at low frequency, $f = \omega/N_{ac} = 0.5$, in a weak magnetic field perpendicular to the B_o - g plane, $\phi = 90^o$.

(b) Imaginary part of k_z along the same slice. Units are H^{-1}.

Fig. 13 (a) Wave vector surface of "slow gravity mode" at low frequency, $f = /N_{ac} = 0.5$, in a moderate magnetic field.

(b) Wave vector surface of magnetic "fast" mode in same case. Full scale along each axis is $\pm$ 1/H.

Fig. 14 Wave vector surface at low frequency, $f = \omega/N_{ac} = 0.5$, in a strong magnetic field. Bulge is magnetic pressure fast mode. Other mode is a plane through origin. Full scale along each axis is $\pm$ 0.1/H.

Fig. 15 (a) Slice through wave vector surface at low frequency, $f = \omega/N_{ac} = 0.5$, in a strong field.

(b) Imaginary part of k_z along the same slice. Units are H^{-1}.

Fig. 16 (a) Slice through wave vector surface at low frequency, $f = \omega/N_{ac} = 0.5$, in a strong magnetic field, in a direction perpendicular to the $\underset{\sim}{B}_o$-g plane, $\phi = 90^o$.

(b) Imaginary part of k_z along the same slide. Units are H^{-1}.

Fig. 17 (a) Slice through the wave vector surface at low frequency $f = \omega/N_{ac} = 0.5$, in a nearly vertical, $\theta = 5^o$, strong magnetic field.

(b) Imaginary part of k_z along the same slice. Units are H^{-1}.

Fig. 18 Wave vector surface for nearly horizontal magnetic field, $\theta = 85^o$, at frequency, $f = \omega/N_{ac} = 0.5$, in a moderate magnetic field. The cutoff frequency in this case is $N_{ac}\, s/(s^2 + a^2)^{\frac{1}{2}} = 0.58\, N_{ac}$. The inner fast mode surface is similar to the magneto-gravity mode surface. (Schwartz and Stein, 1975 fig. 3b).

Fig. 19 Hexagonal planform f(x,y).

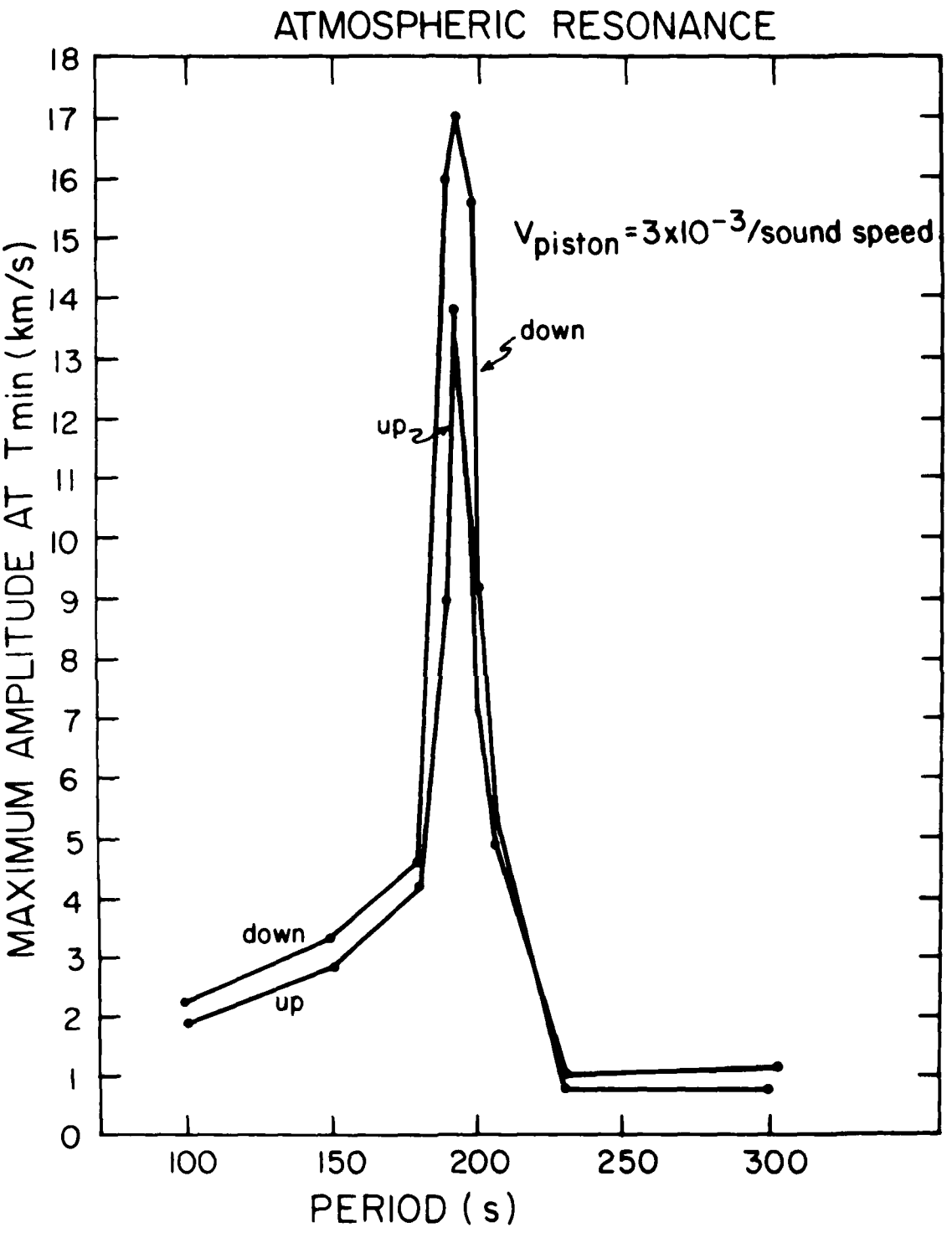
ATMOSPHERIC RESONANCE
MAXIMUM AMPLITUDE AT Tmin (km/s)
PERIOD (s)
$V_{piston} = 3 \times 10^{-3}$/sound speed
down
up
down
up
0
1
2
3
4
5
6
7
8
9
10
11
12
13
14
15
16
17
18
100
150
200
250
300

Figure 1

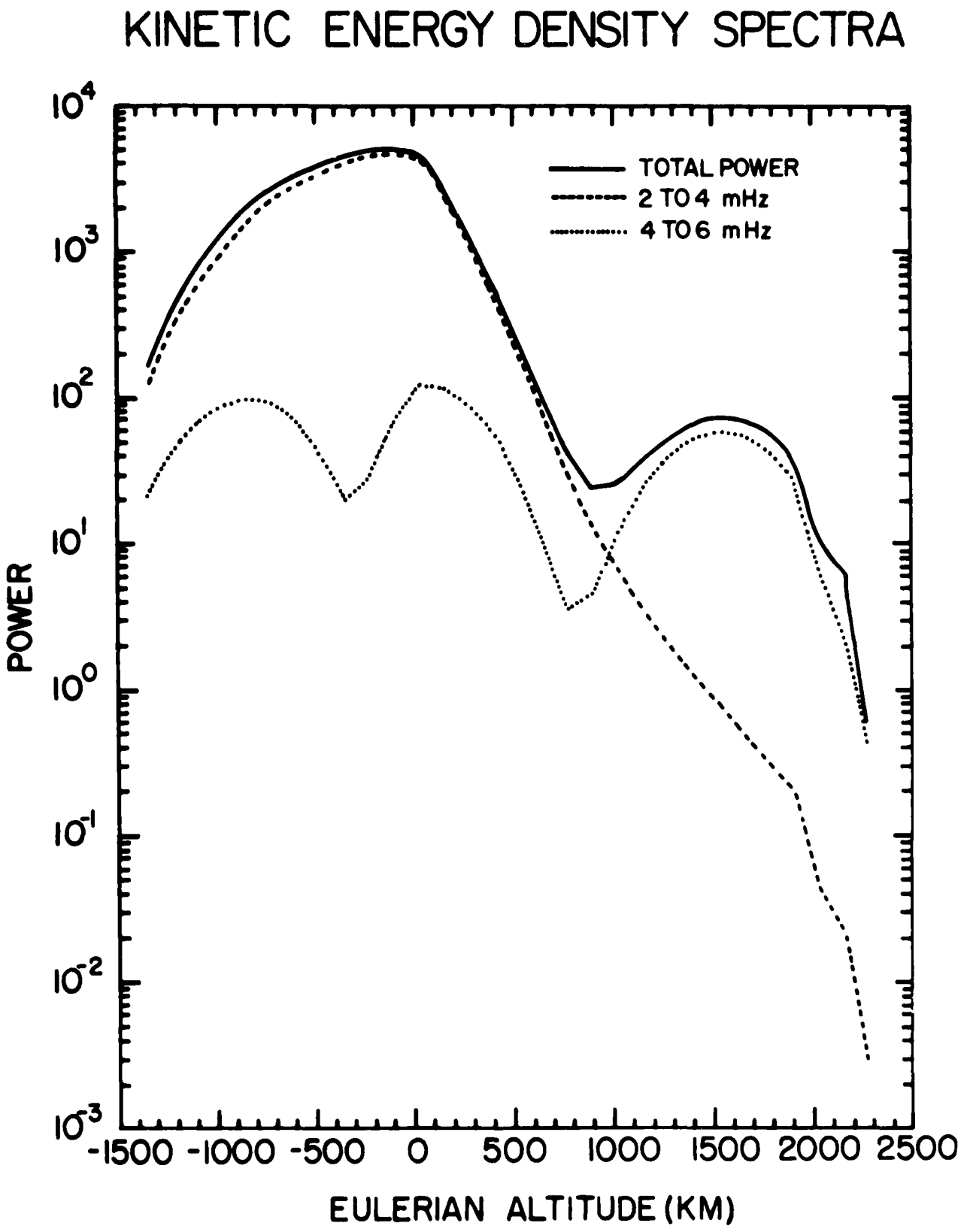
KINETIC ENERGY DENSITY SPECTRA
TOTAL POWER
2 TO 4 mHz
4 TO 6 mHz
POWER
10^4
10^3
10^2
10^1
10^0
10^{-1}
10^{-2}
10^{-3}
-1500 -1000 -500 0 500 1000 1500 2000 2500
EULERIAN ALTITUDE (KM)

Figure 2

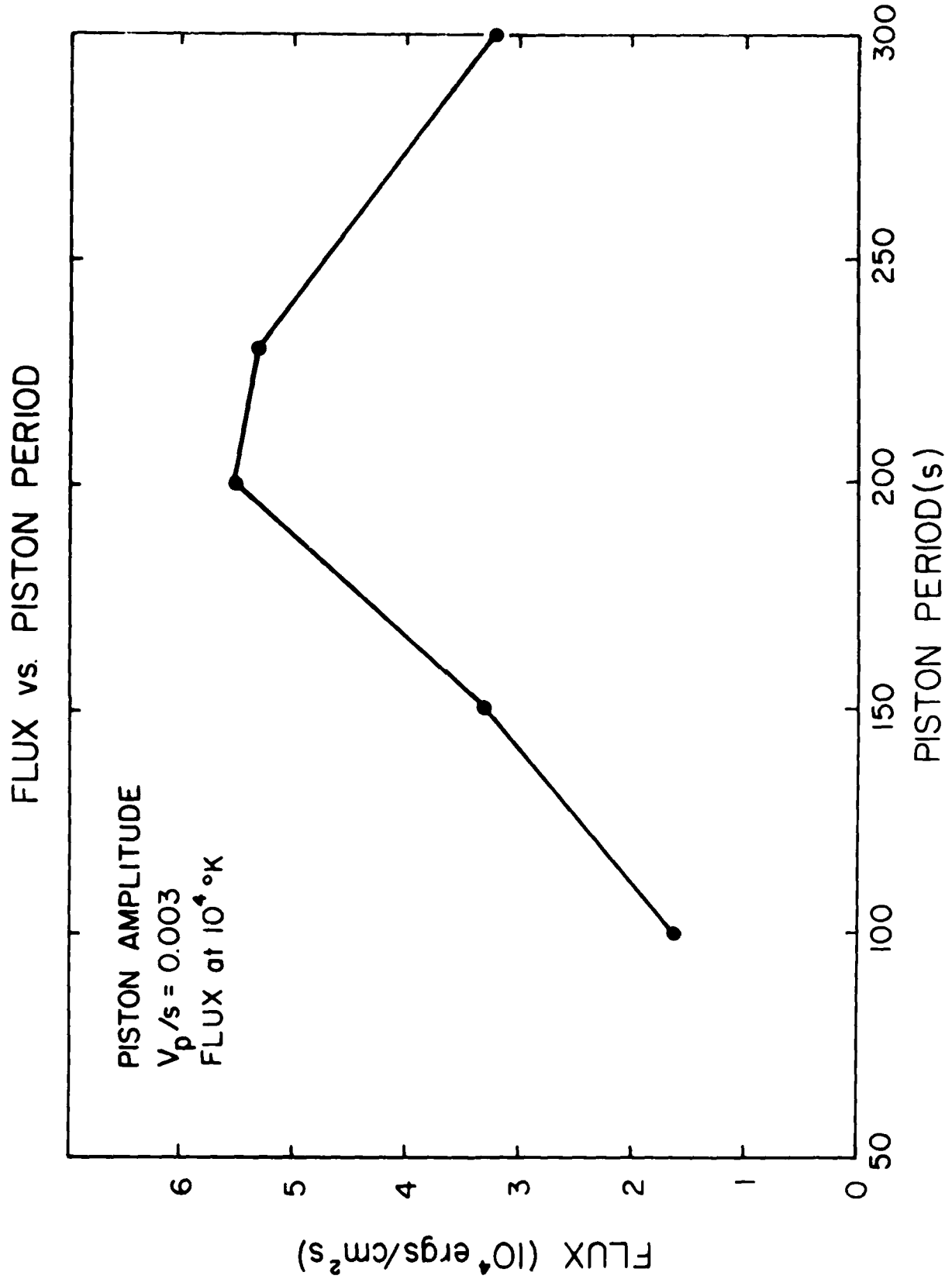
FLUX vs. PISTON PERIOD
PISTON AMPLITUDE
$V_p/s = 0.003$
FLUX at 10^4 °K
FLUX (10^4 ergs/cm^{2}s)
PISTON PERIOD(s)
0
1
2
3
4
5
6
50
100
150
200
250
300

Figure 3

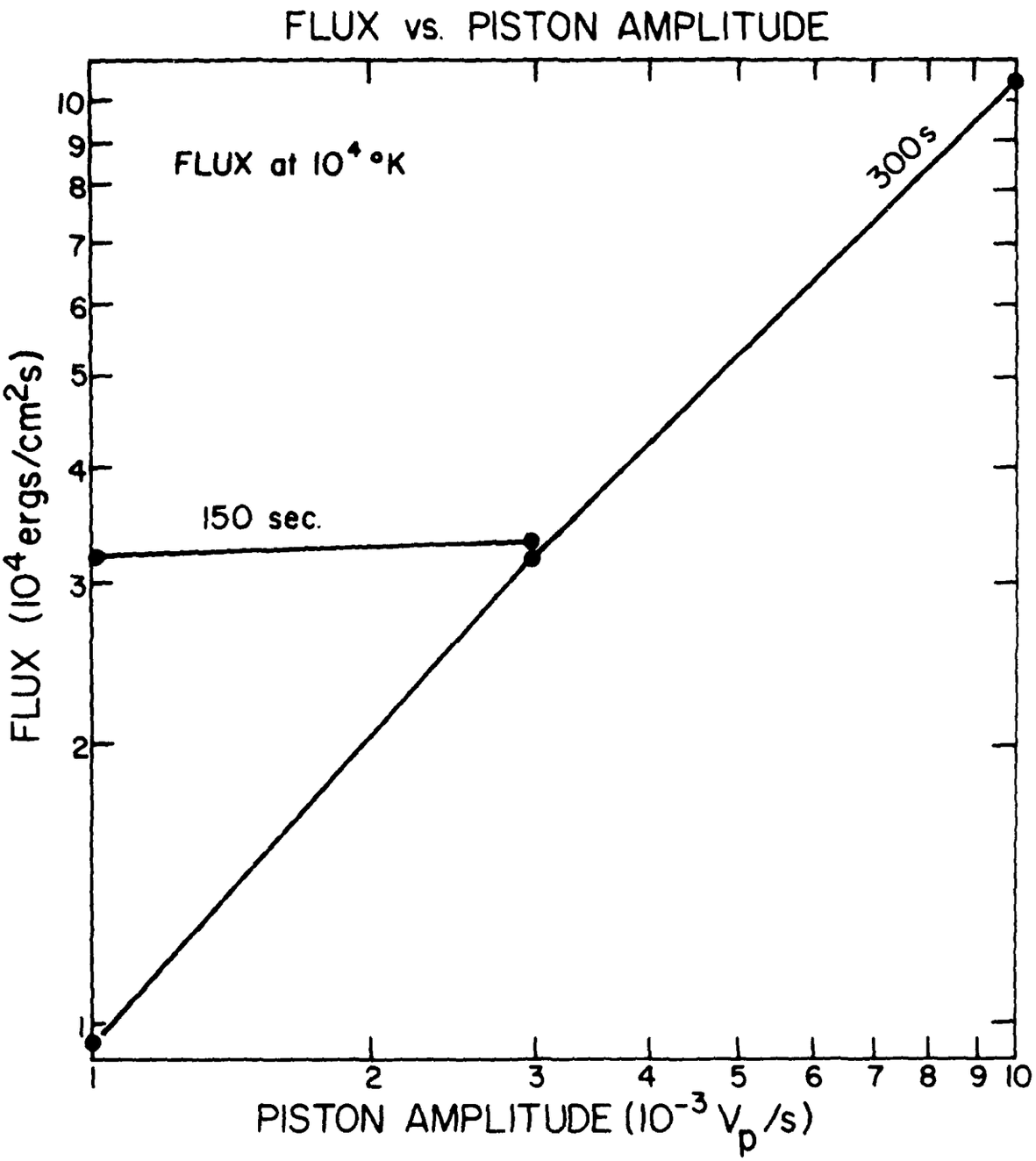
FLUX vs. PISTON AMPLITUDE
FLUX at 10^4 °K
300s
150 sec.
FLUX (10^4 ergs/cm^{2}s)
PISTON AMPLITUDE (10^{-3} V_p/s)
1
2
3
4
5
6
7
8
9
10

Figure 4

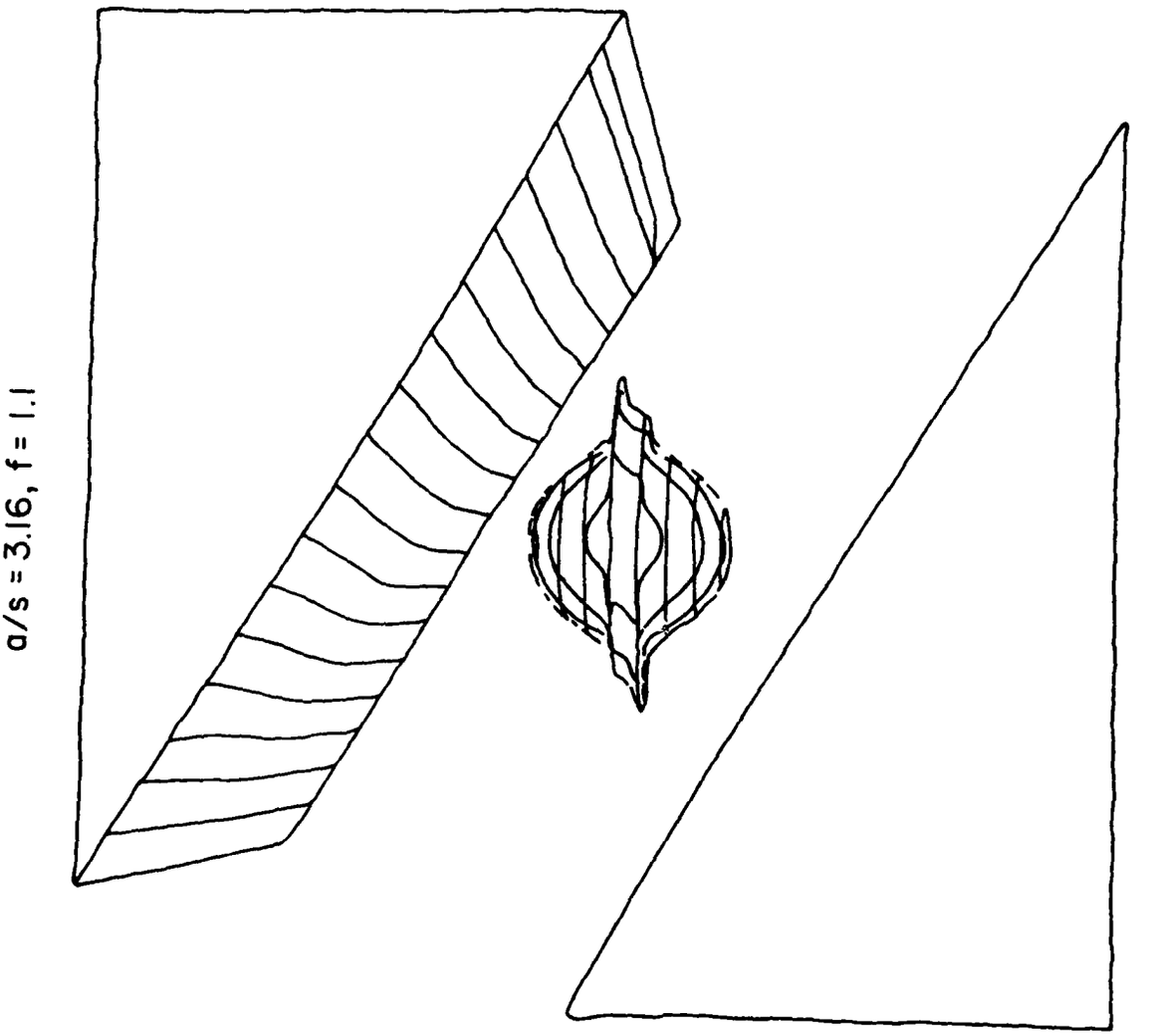

Figure 5

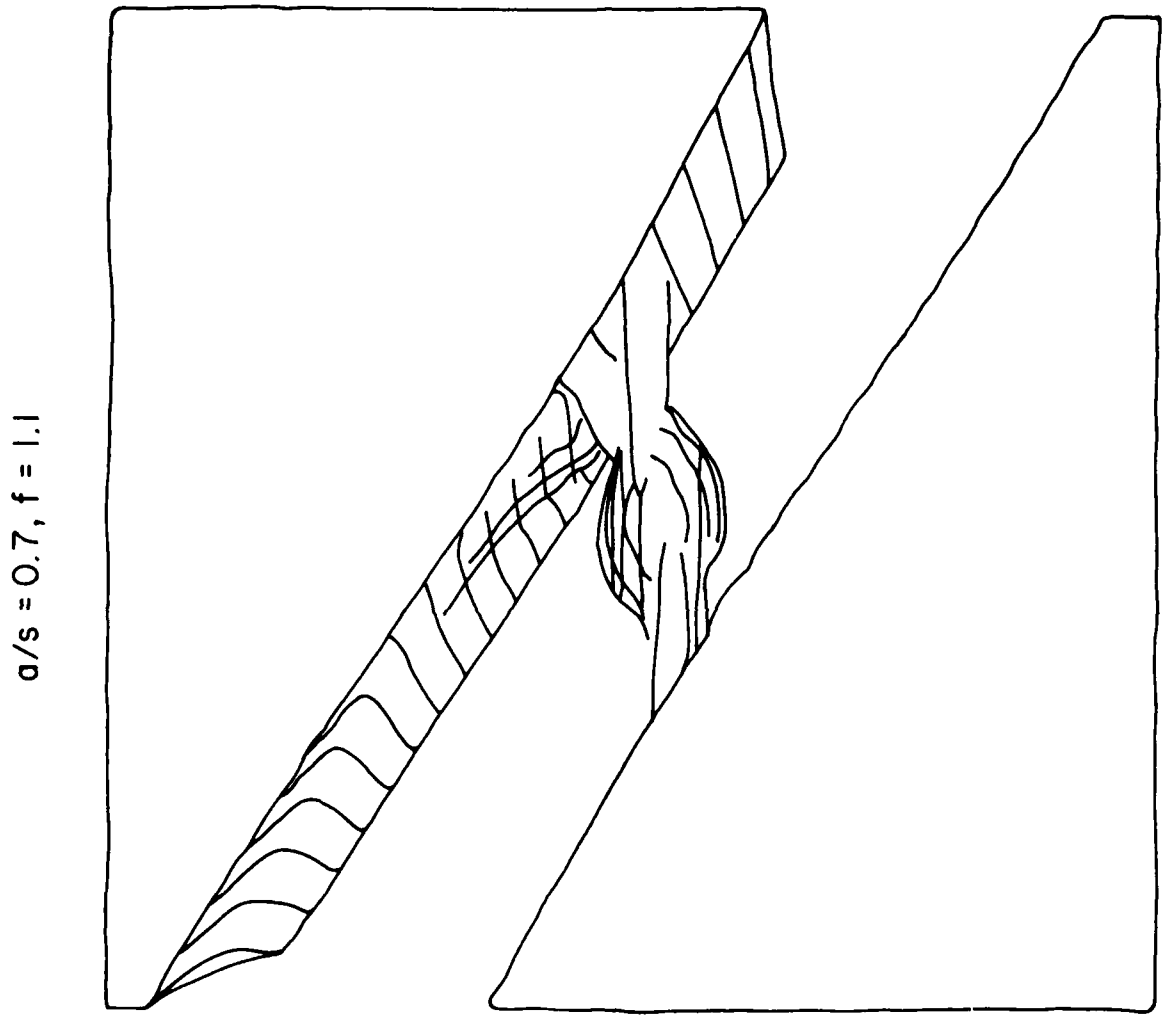

Figure 6

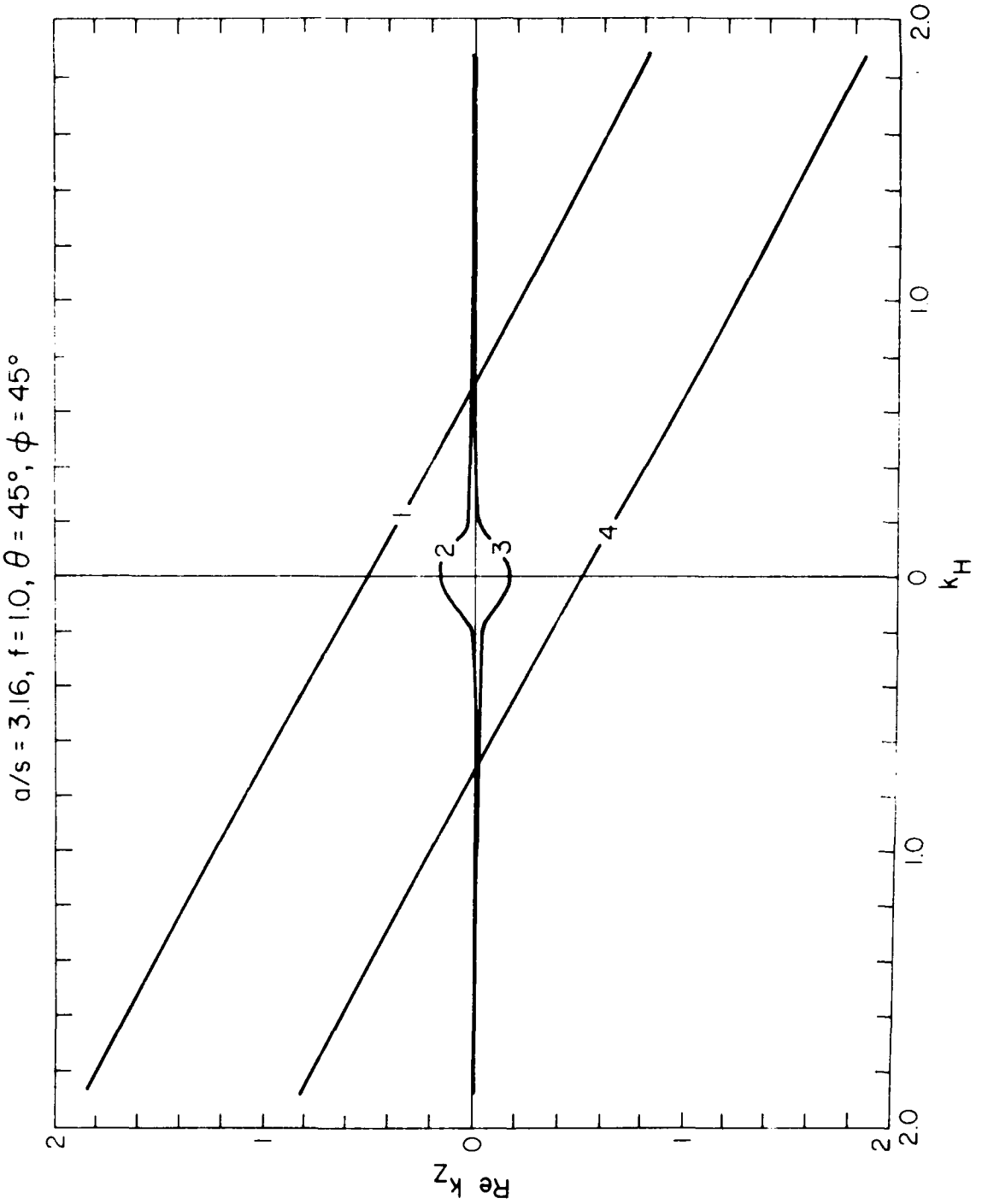

Figure 7

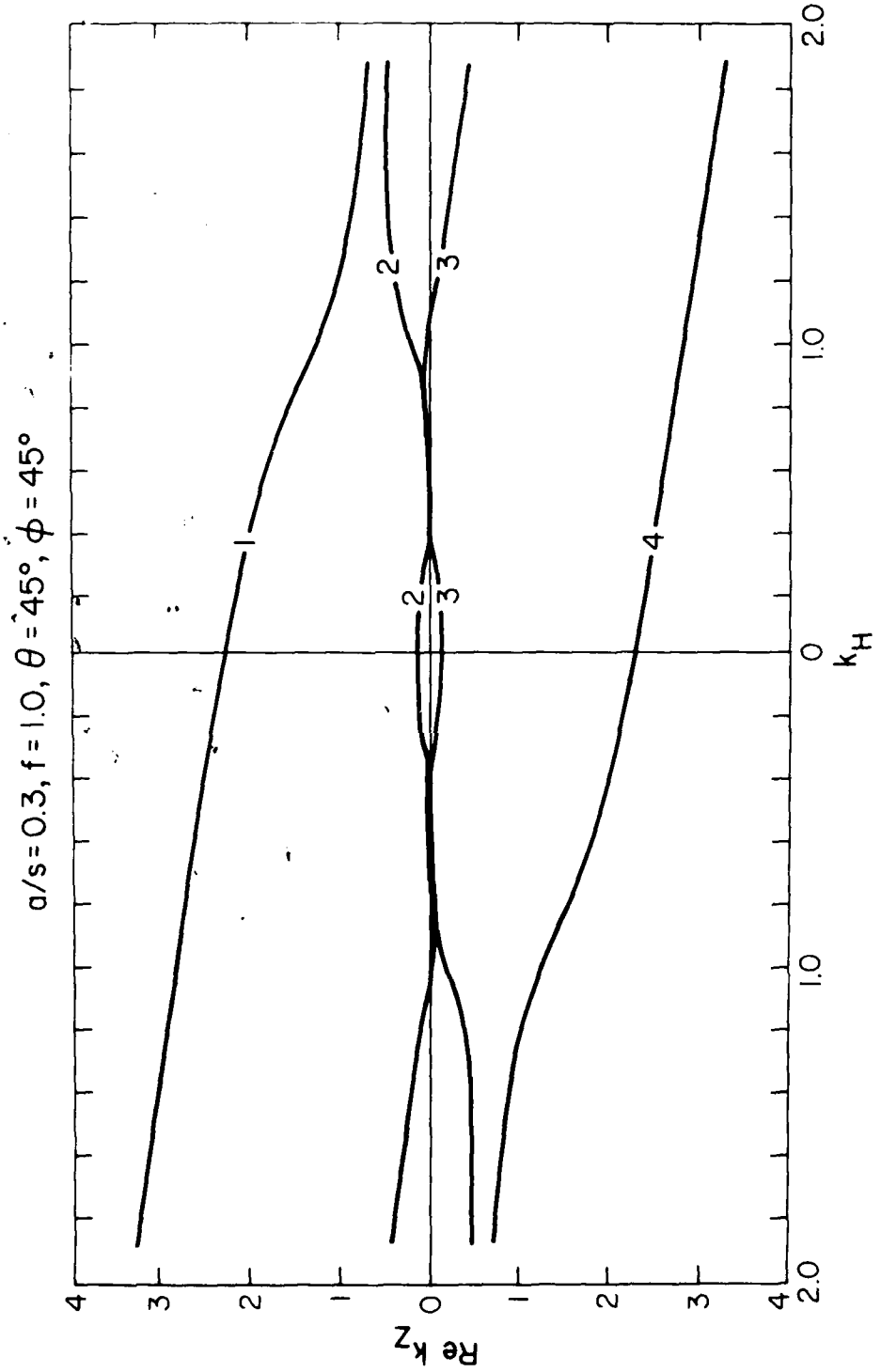

Figure 8a

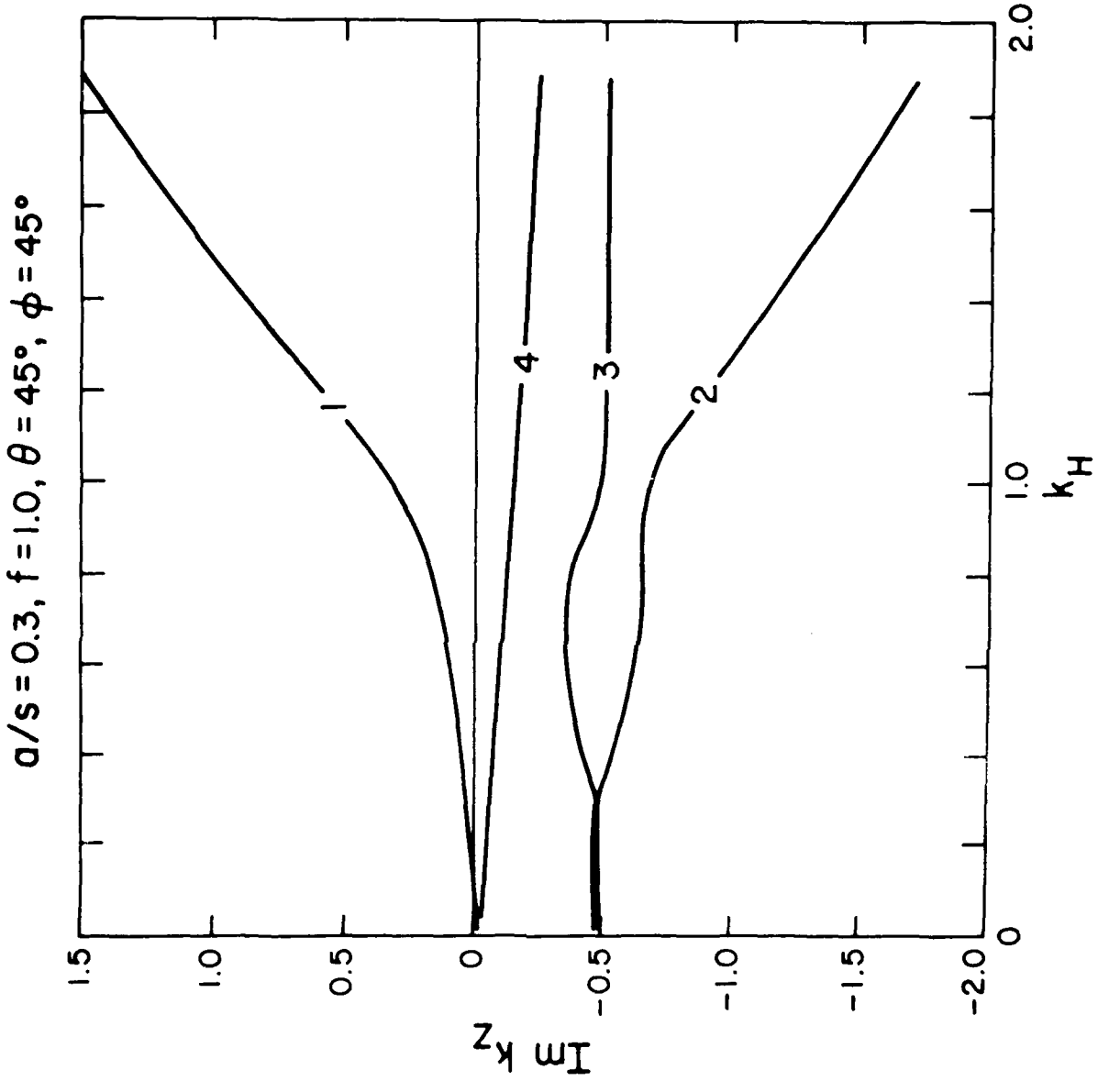

Figure 8b

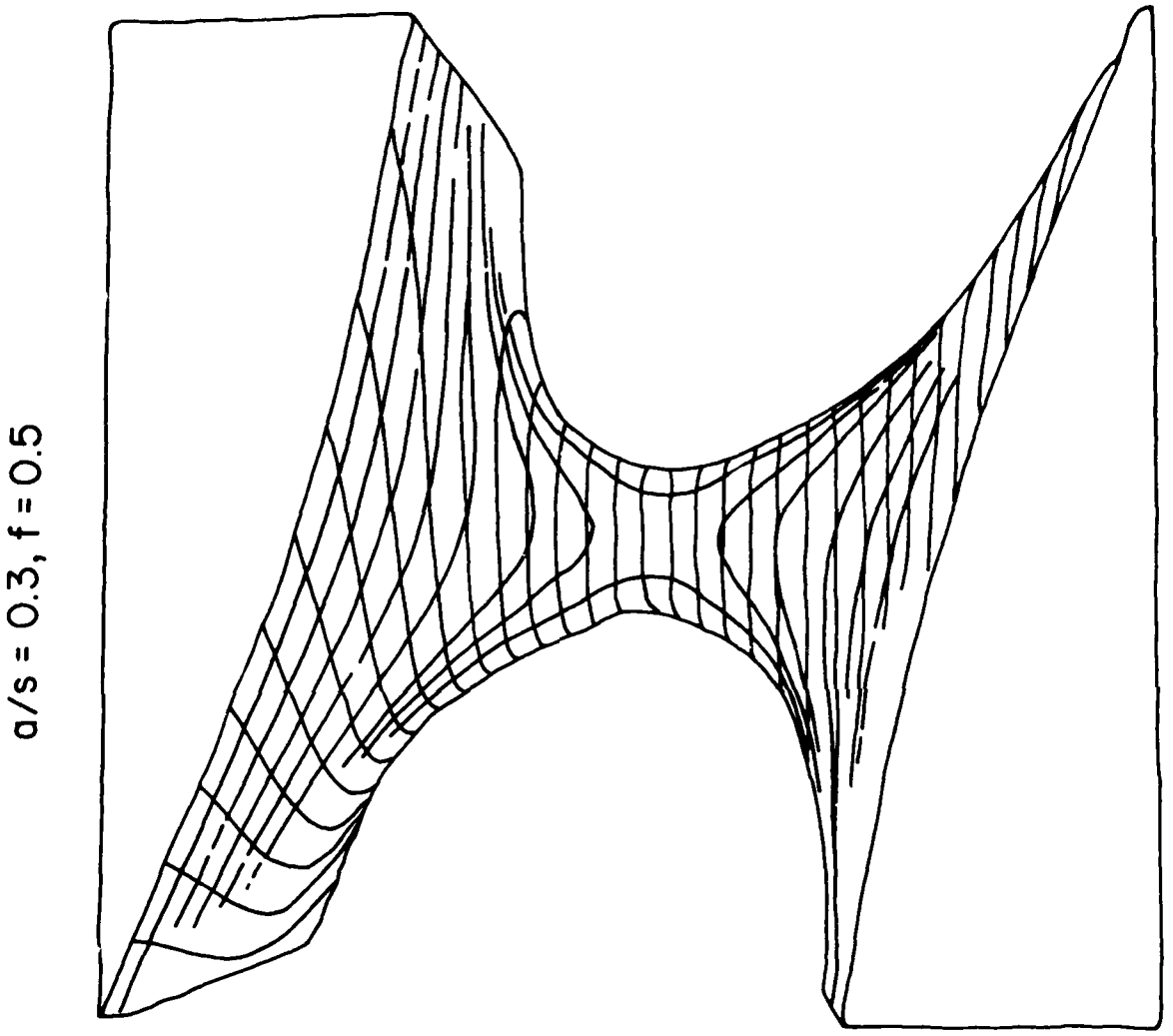

Figure 9a

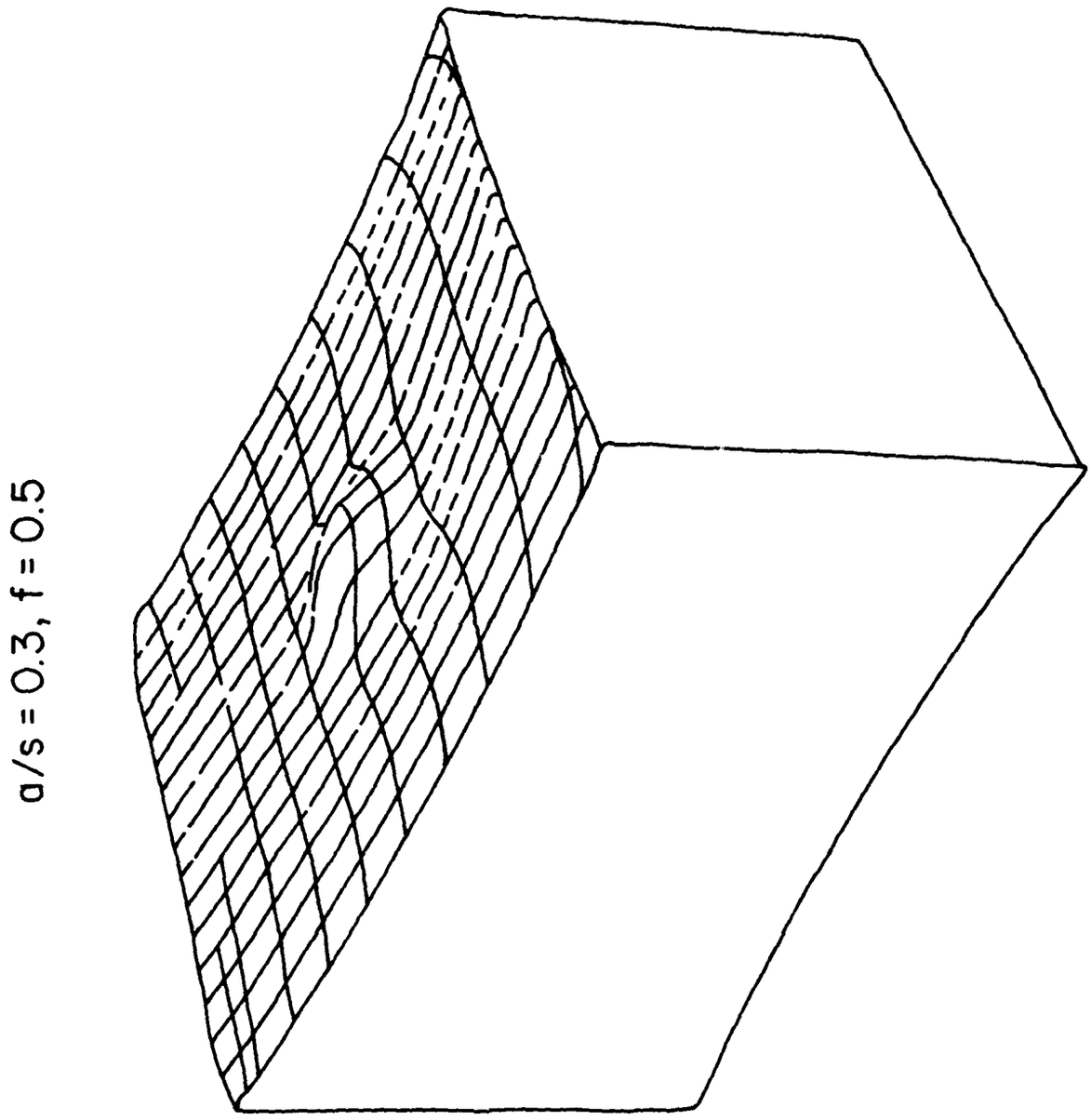

Figure 9b

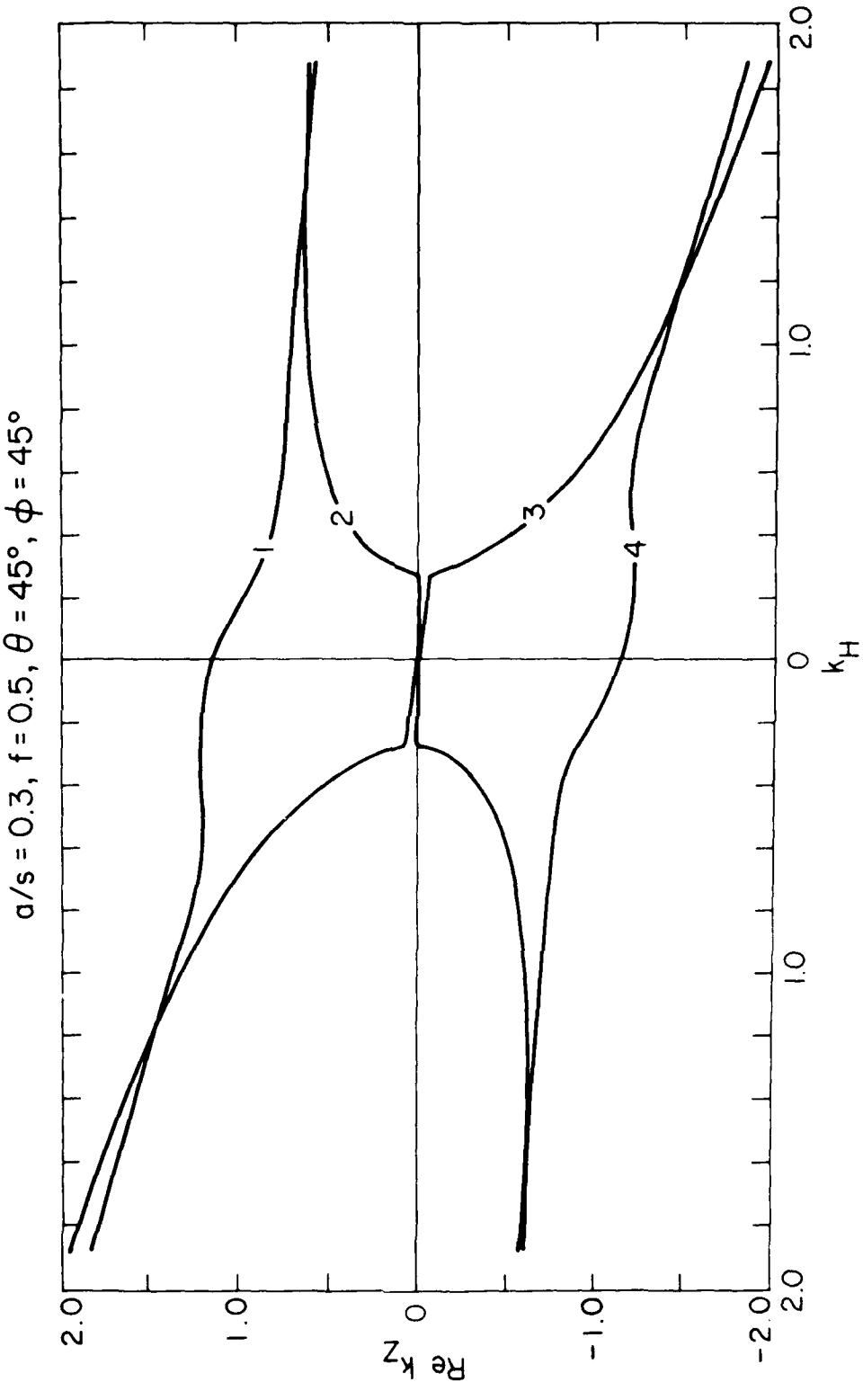

Figure 10a

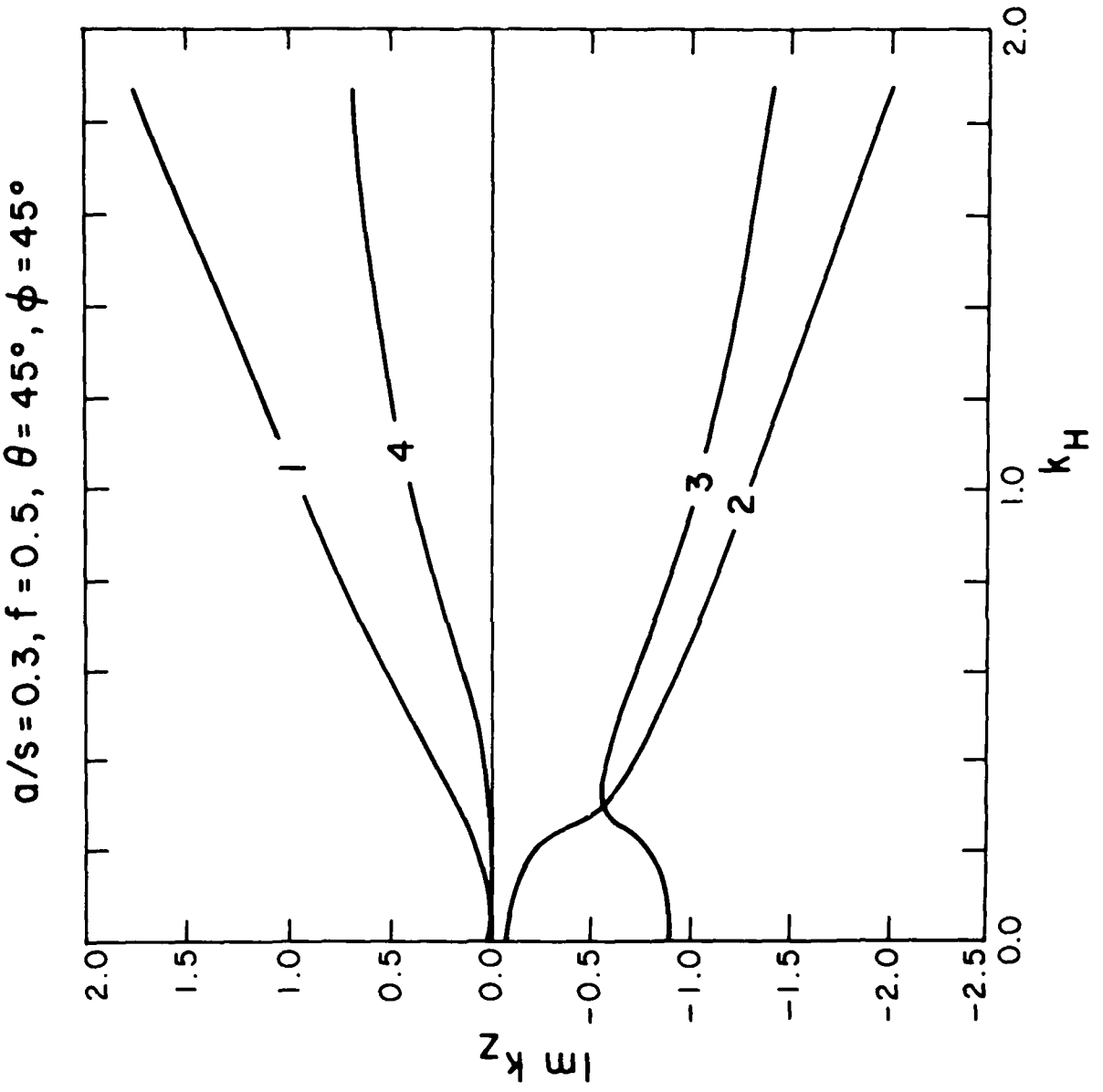

Figures 10b

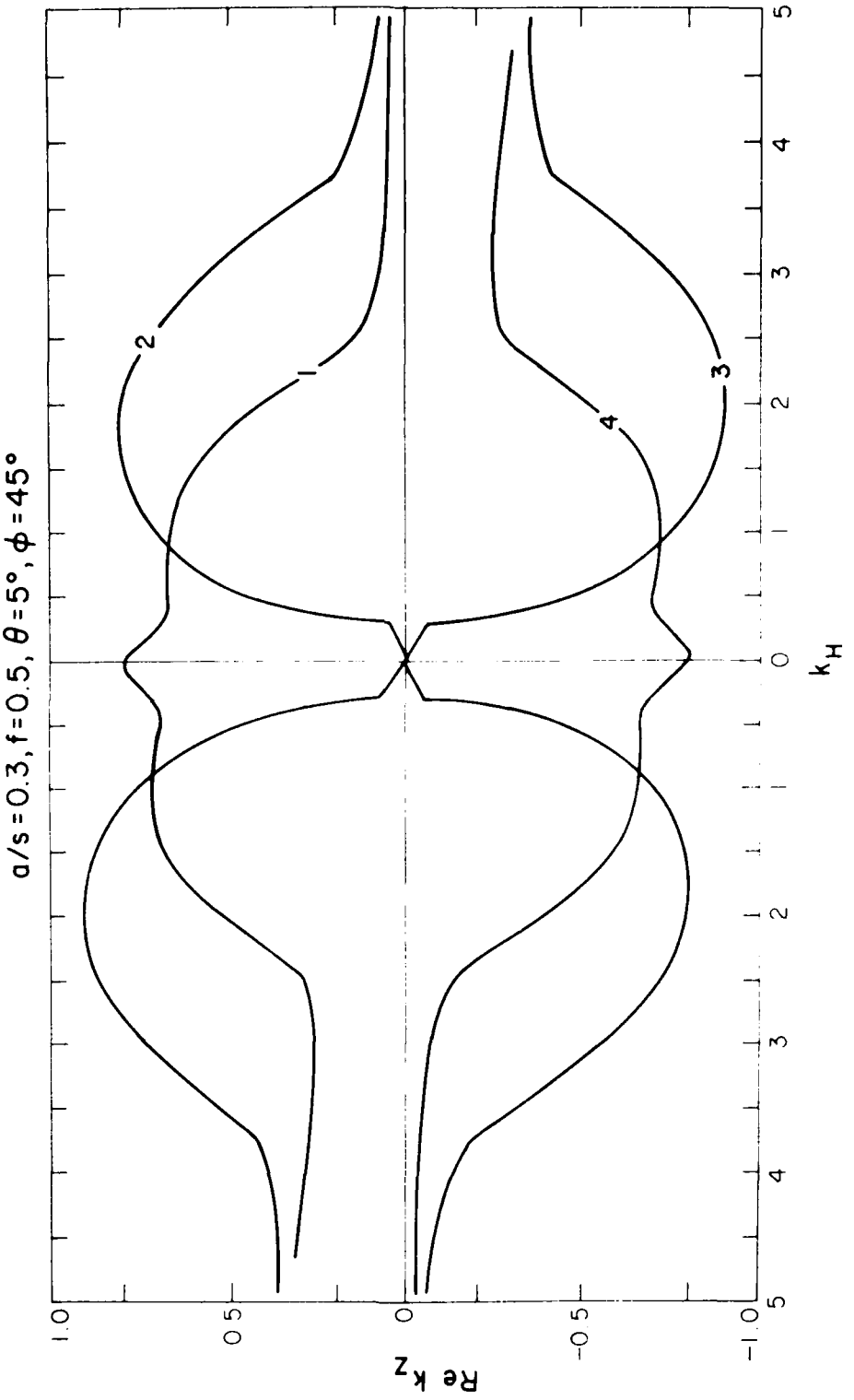

Figure 11a

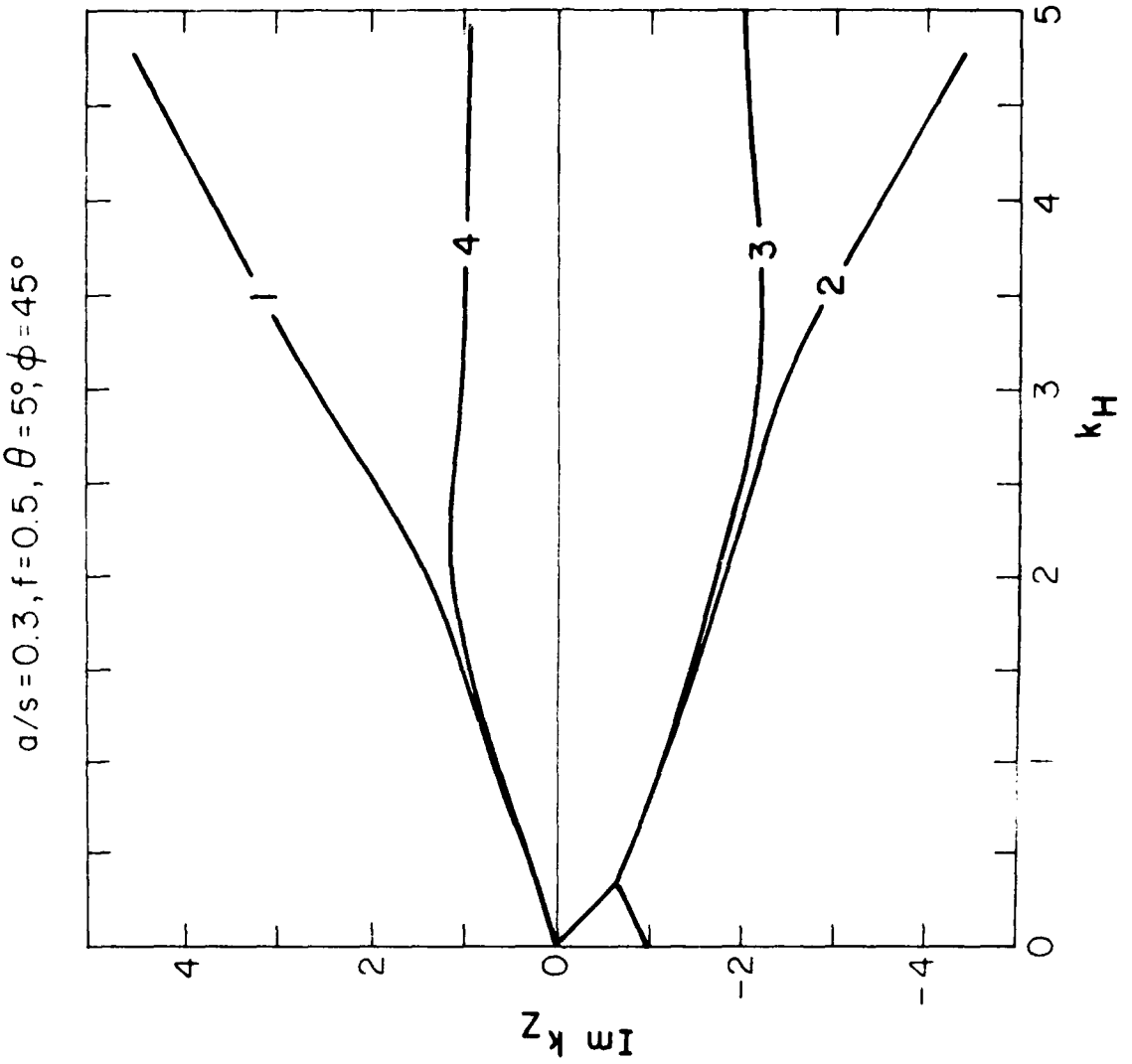

Figure 11b

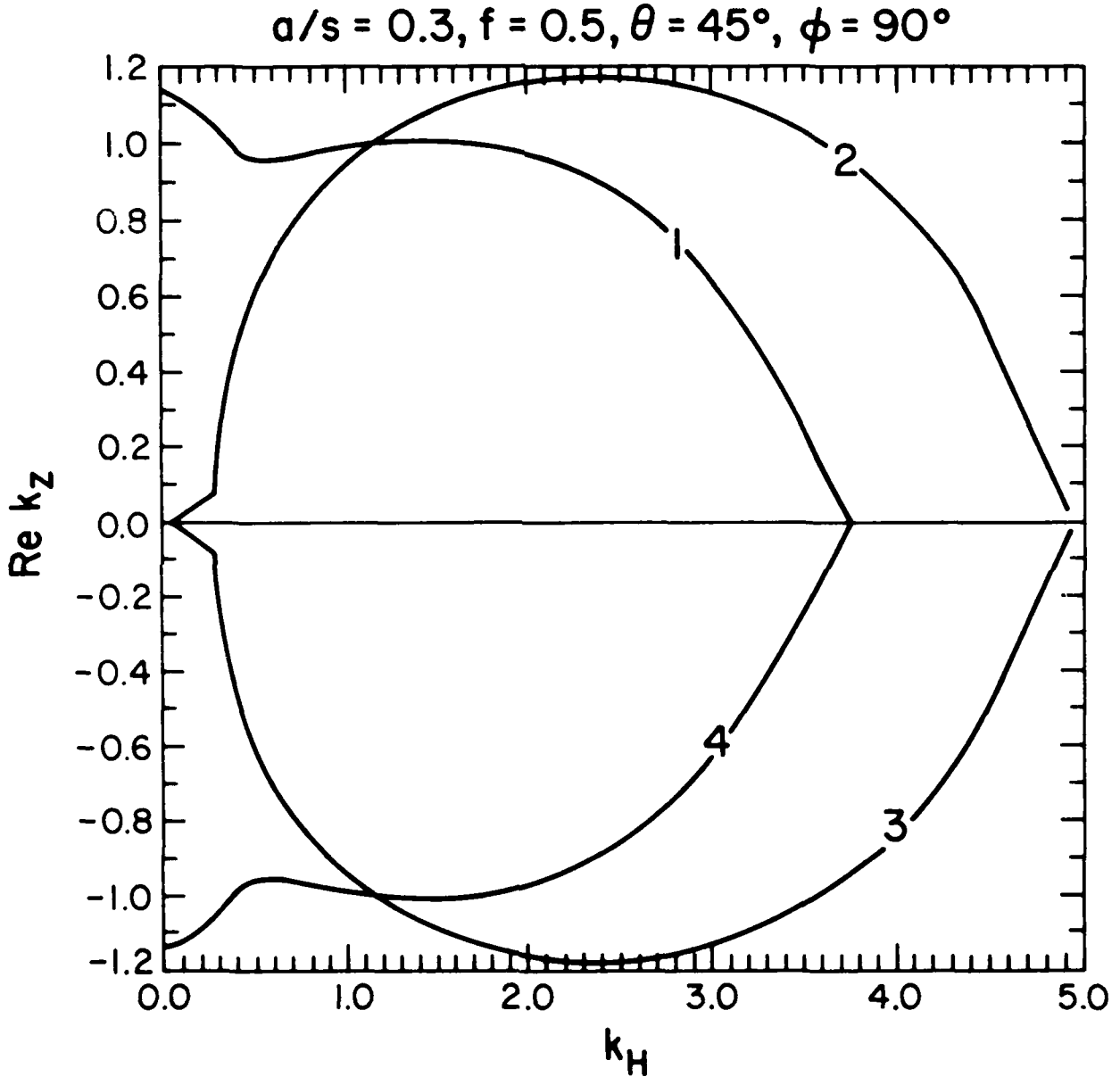
a/s = 0.3, f = 0.5, θ = 45°, φ = 90°
Re k_z
k_H
1.2
1.0
0.8
0.6
0.4
0.2
0.0
-0.2
-0.4
-0.6
-0.8
-1.0
-1.2
0.0
1.0
2.0
3.0
4.0
5.0
1
2
3
4

Figure 12a

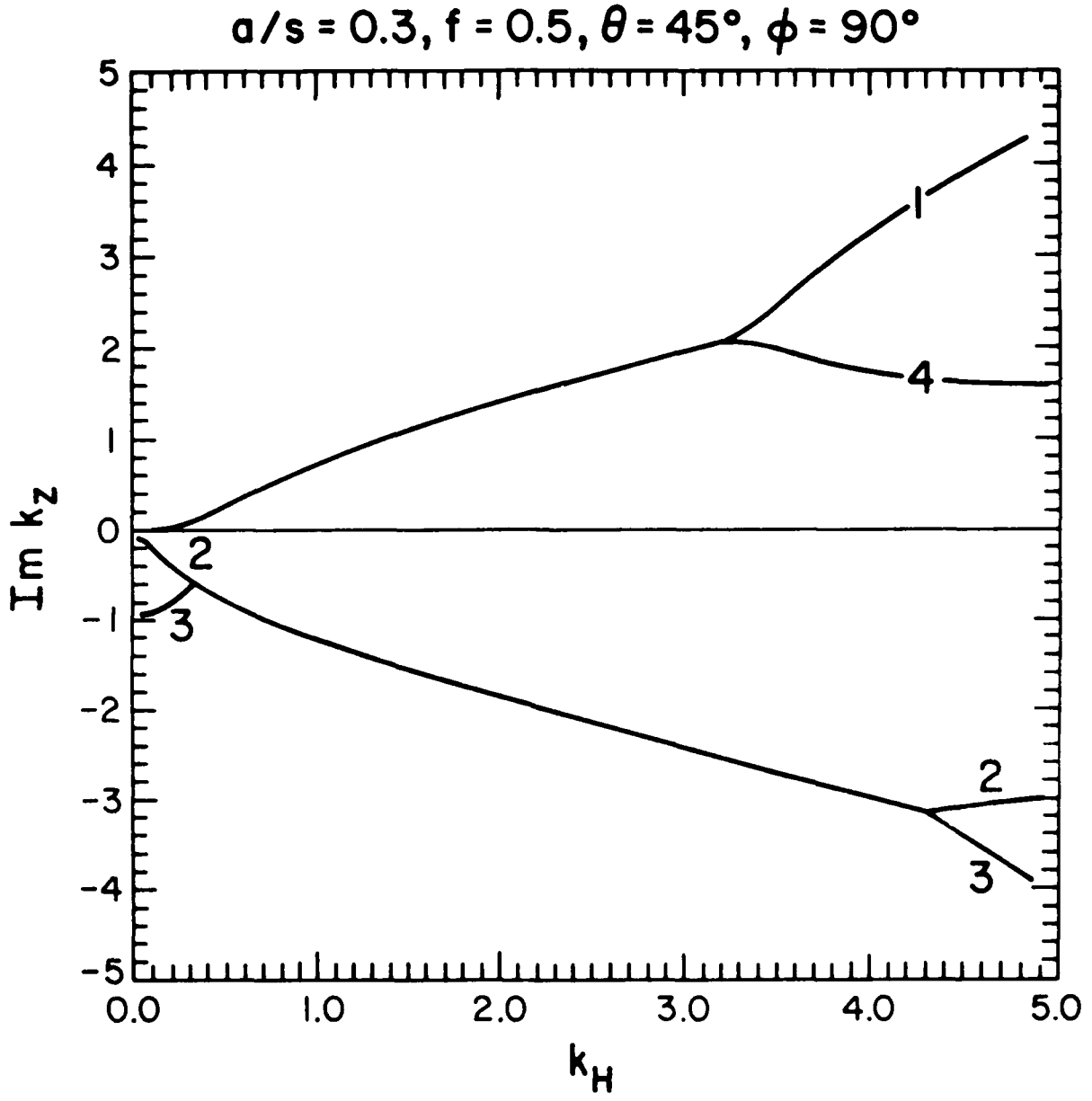

Figure 12b

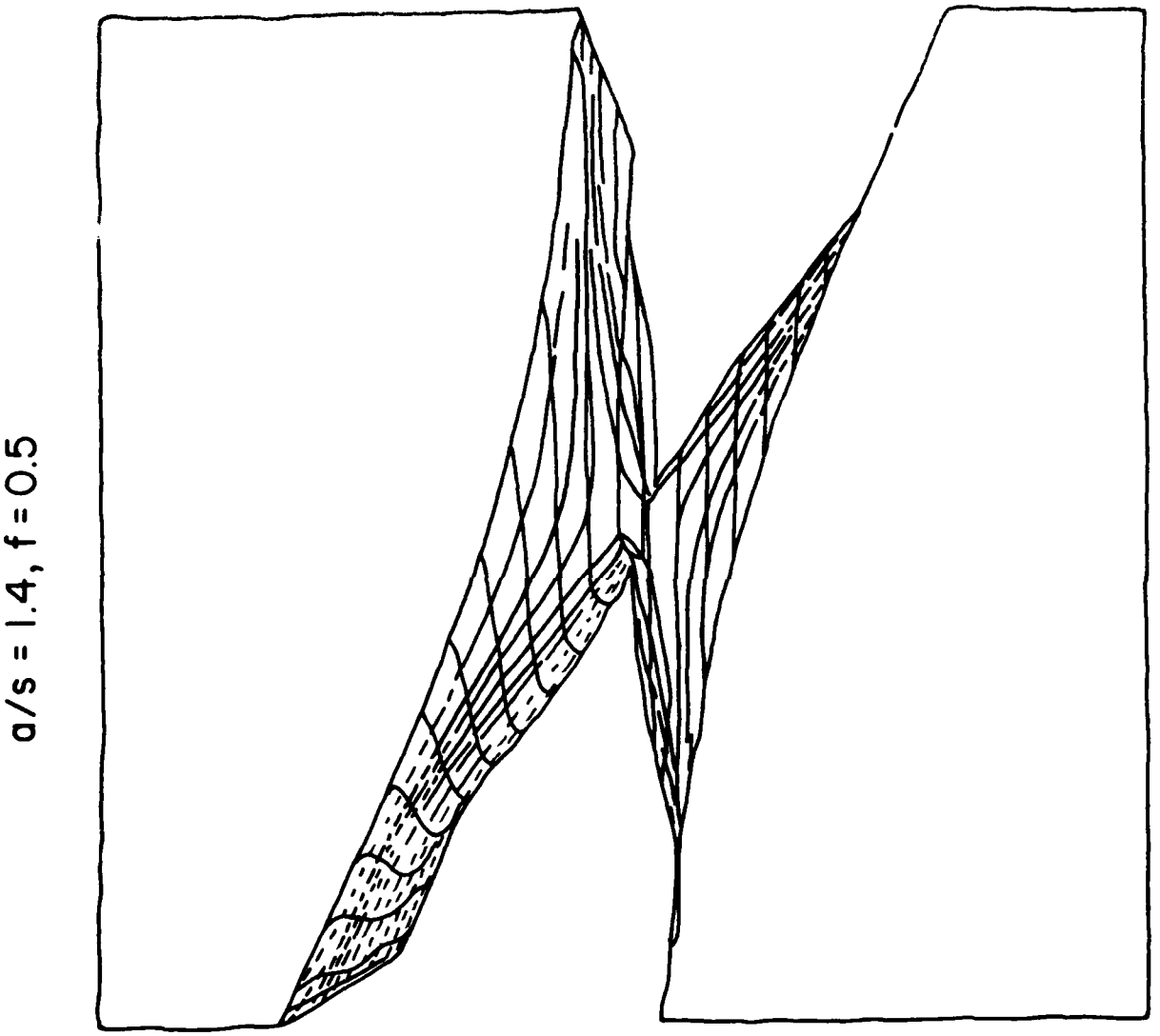

Figure 13a

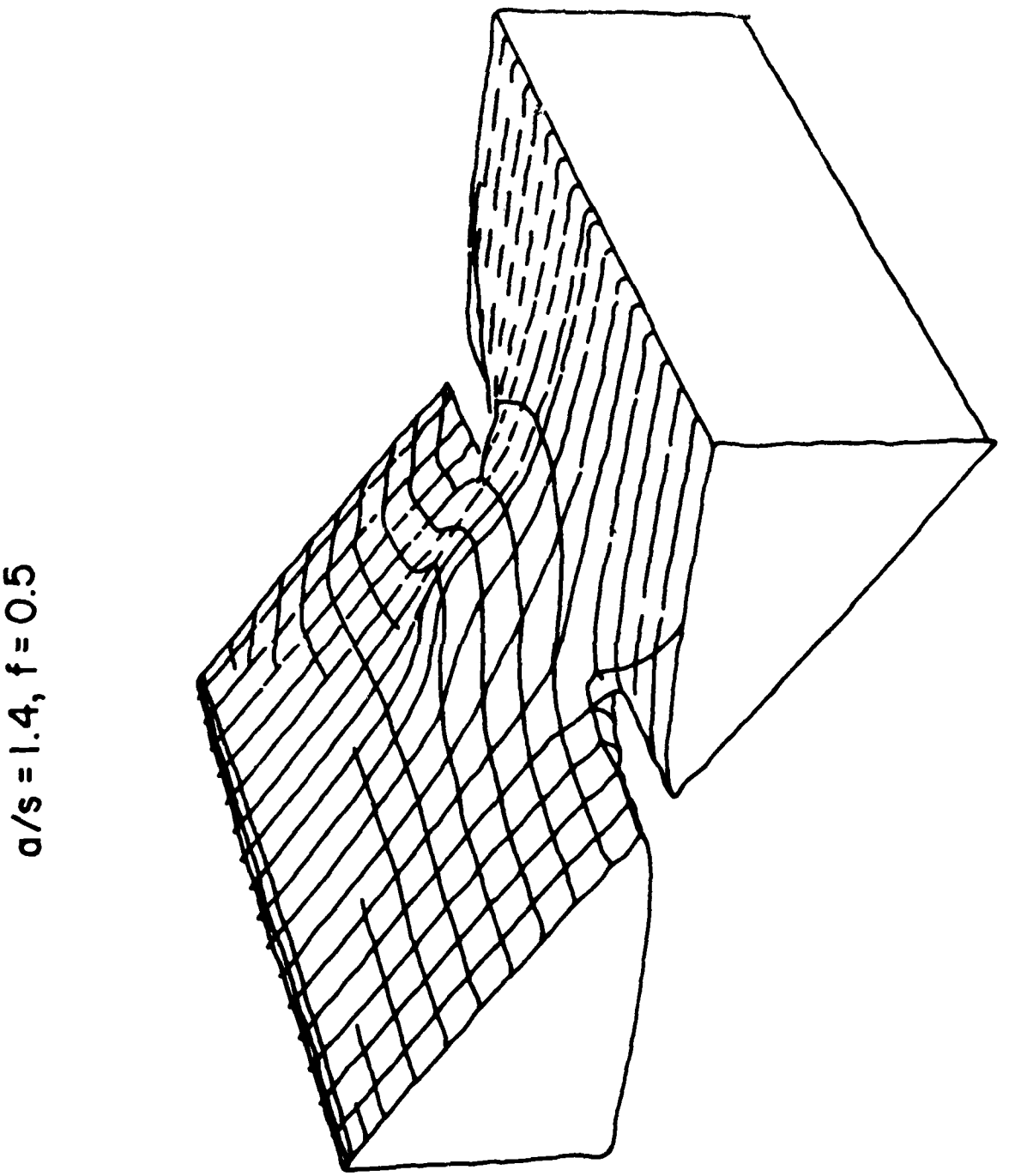

Figure 13b

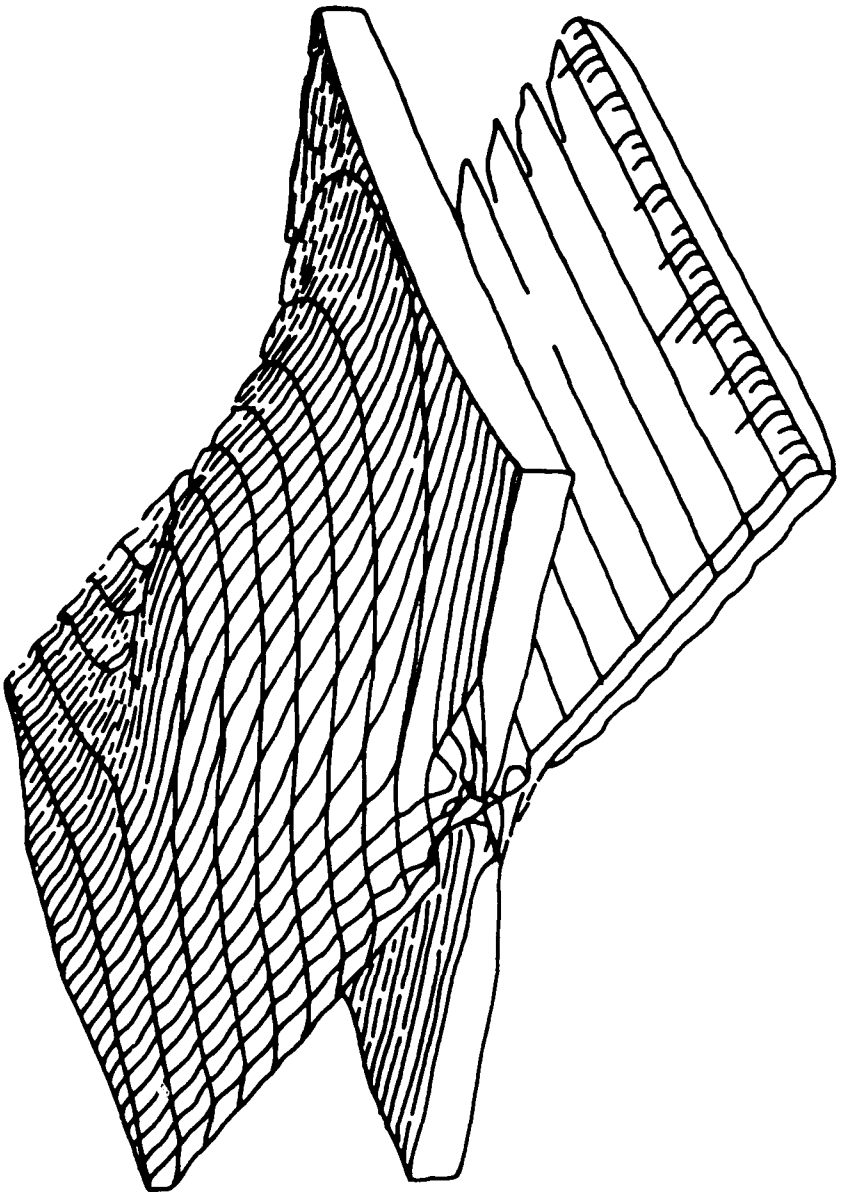

Figure 14

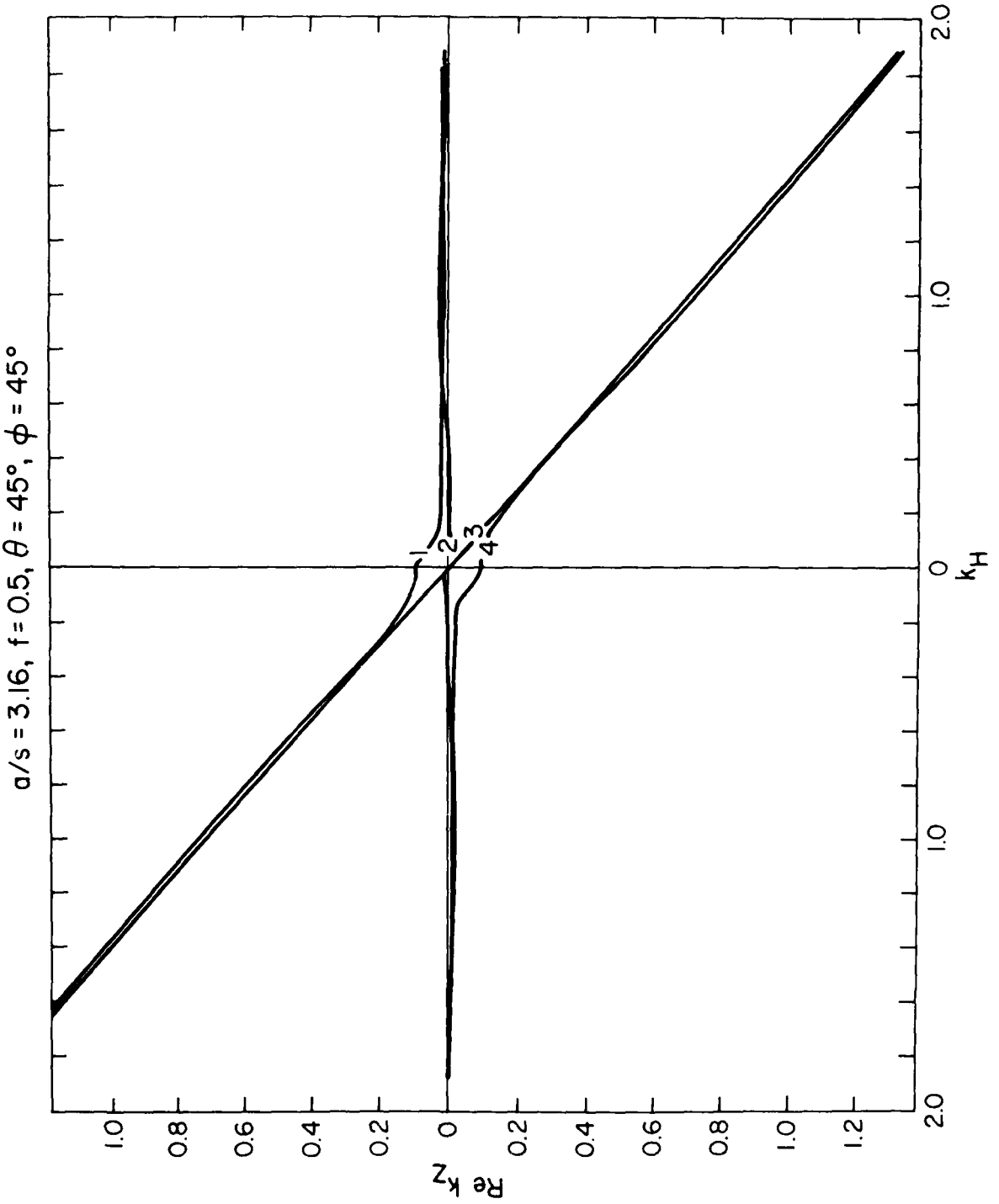
a/s = 3.16, f = 0.5, θ = 45°, φ = 45°
1
2
3
4
Re k_Z
k_H
2.0
1.0
0
1.0
2.0
1.0
0.8
0.6
0.4
0.2
0
0.2
0.4
0.6
0.8
1.0
1.2

Figure 15a

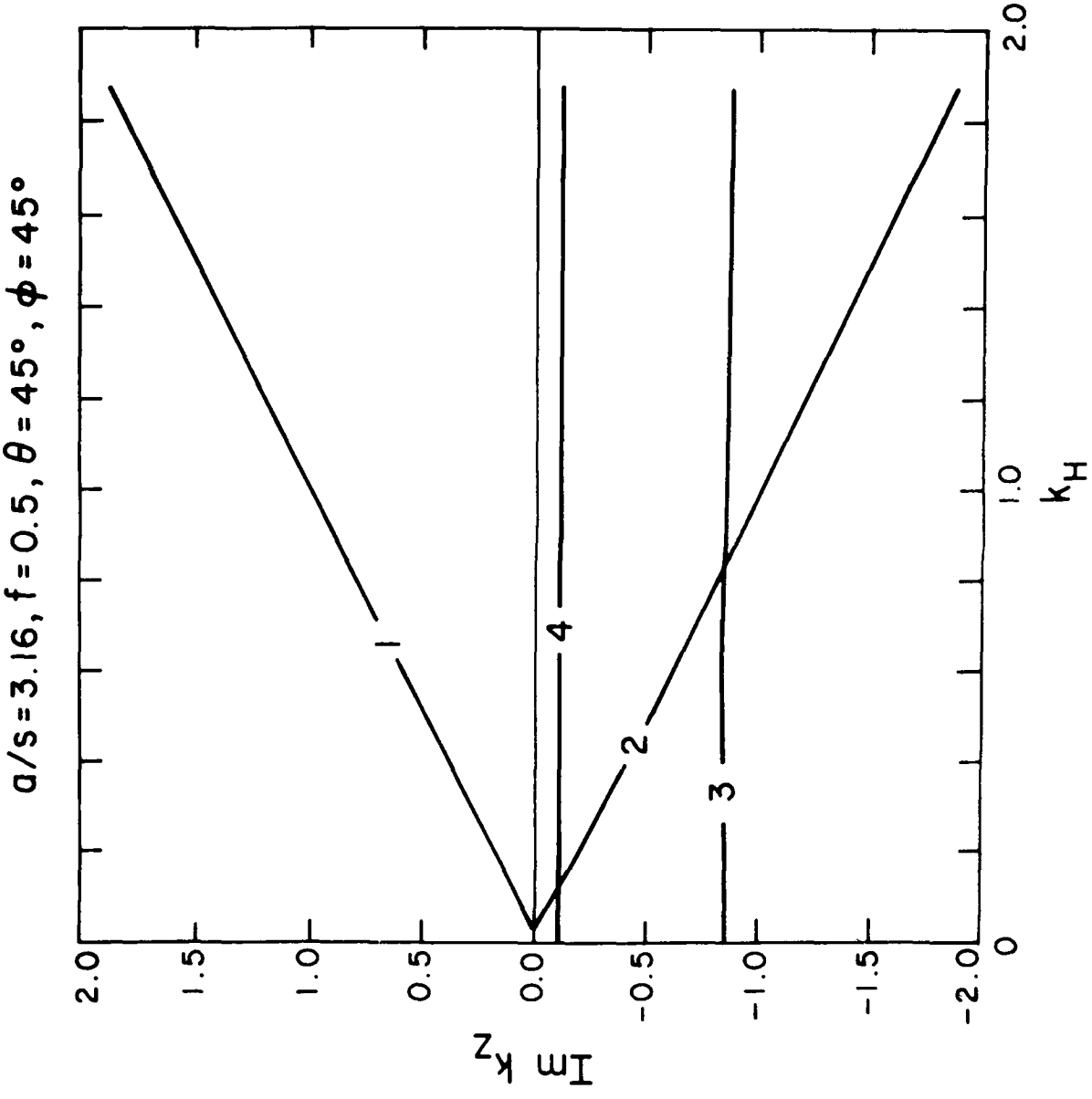

Figure 15b

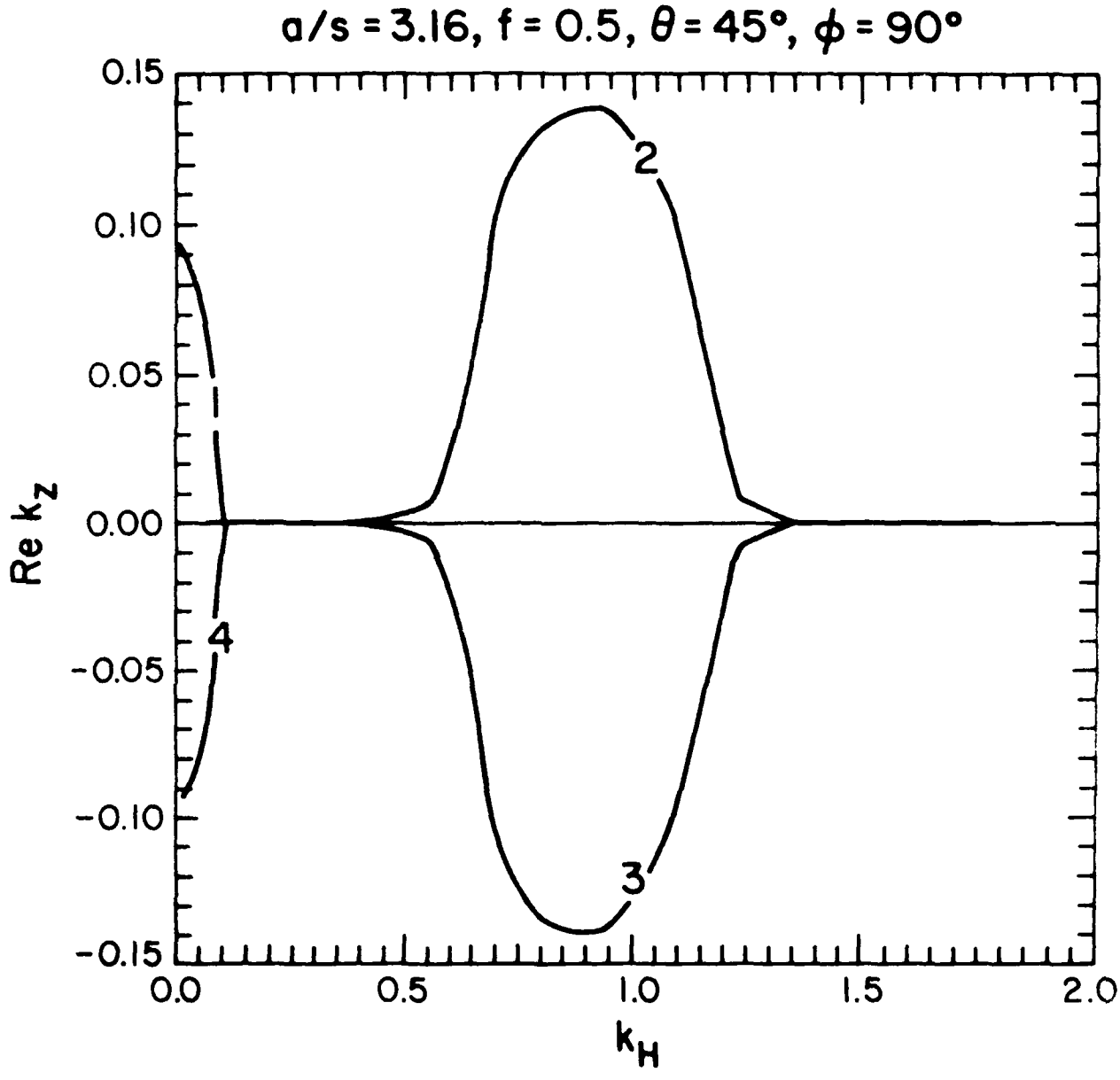
a/s = 3.16, f = 0.5, θ = 45°, φ = 90°
0.15
0.10
0.05
0.00
-0.05
-0.10
-0.15
Re k_z
0.0
0.5
1.0
1.5
2.0
k_H
2
3
4

Figure 16a

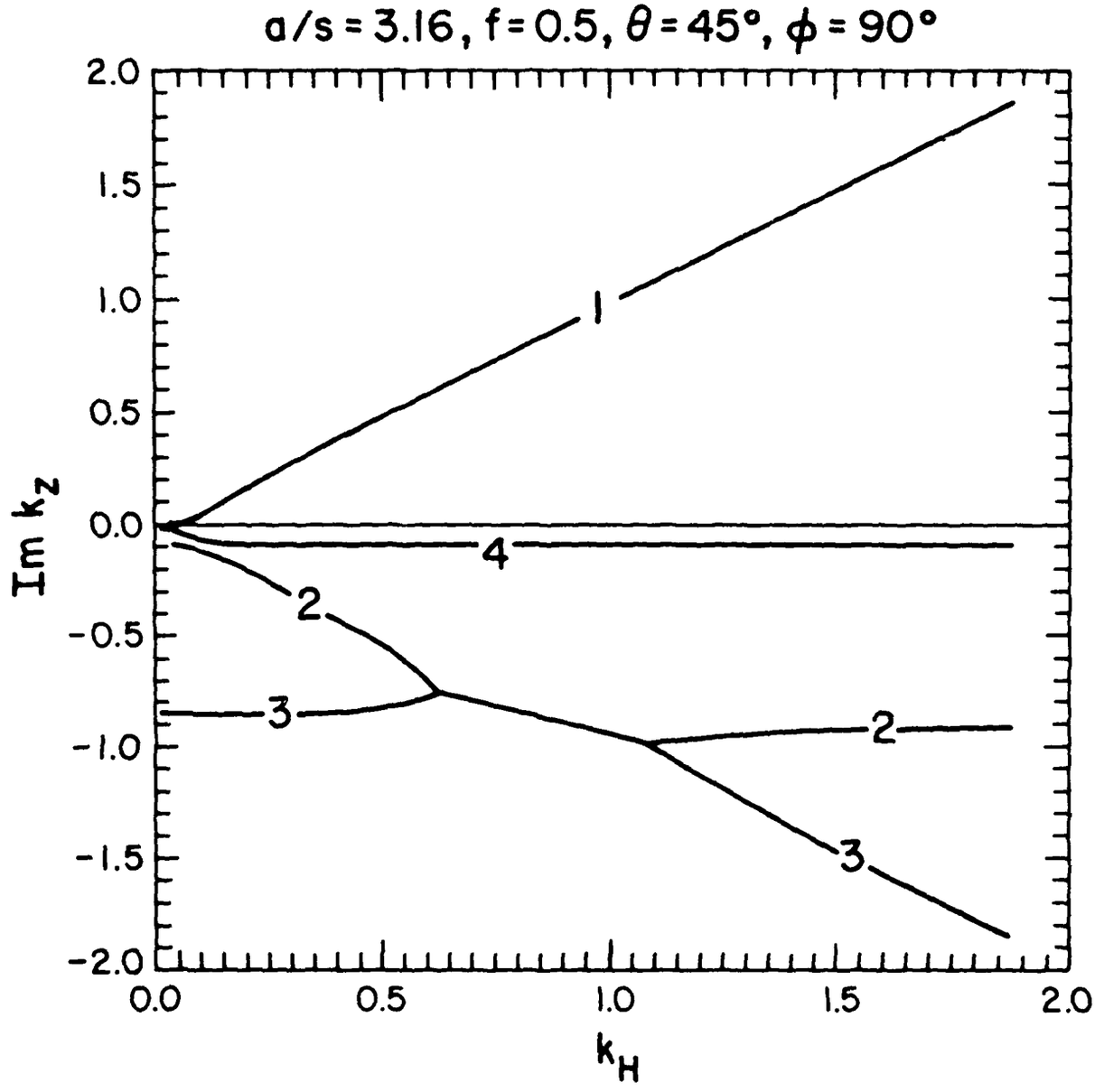
a/s = 3.16, f = 0.5, θ = 45°, φ = 90°
2.0
1.5
1.0
0.5
0.0
-0.5
-1.0
-1.5
-2.0
Im k_z
0.0
0.5
1.0
1.5
2.0
k_H
1
2
3
4
2
3

Figure 16b

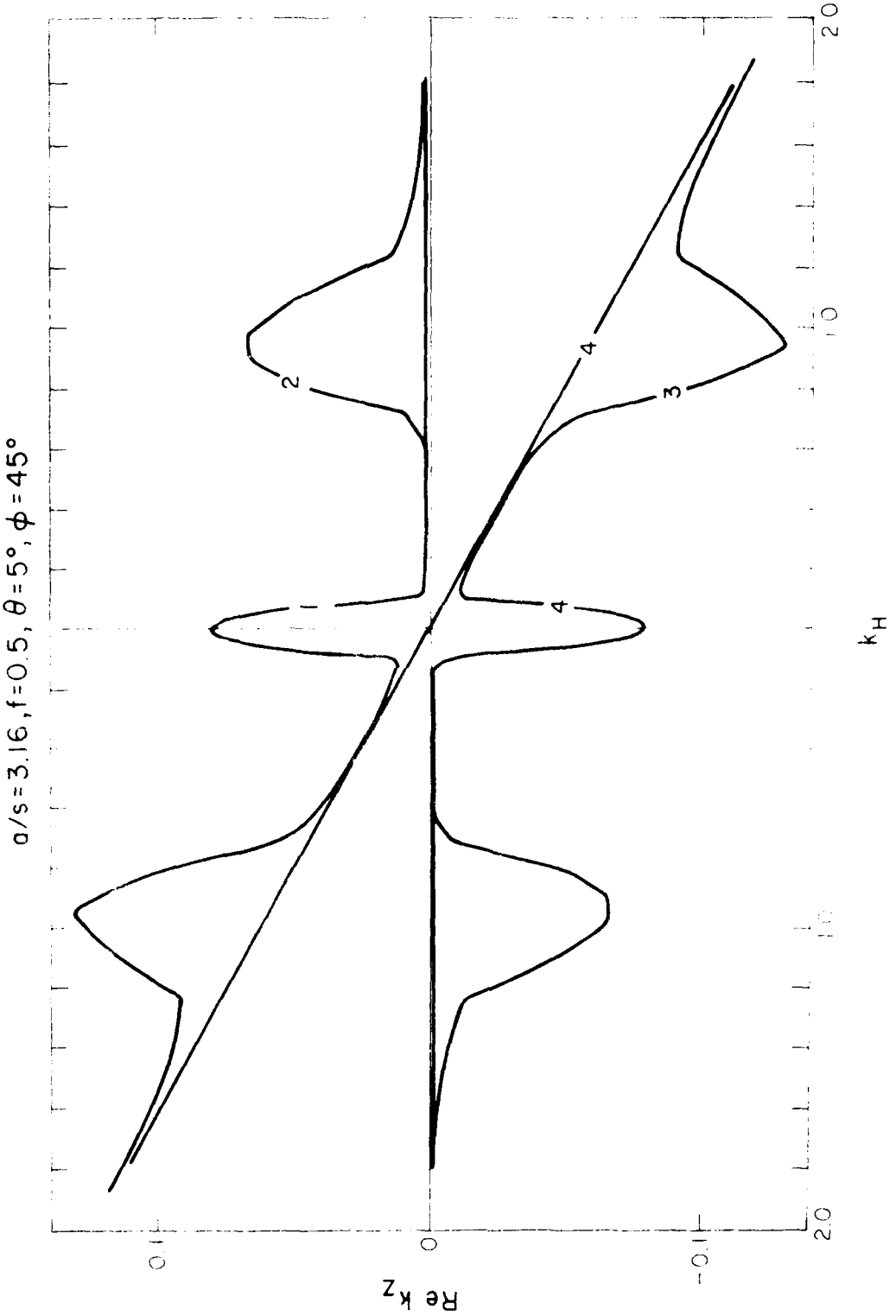

Figure 17a

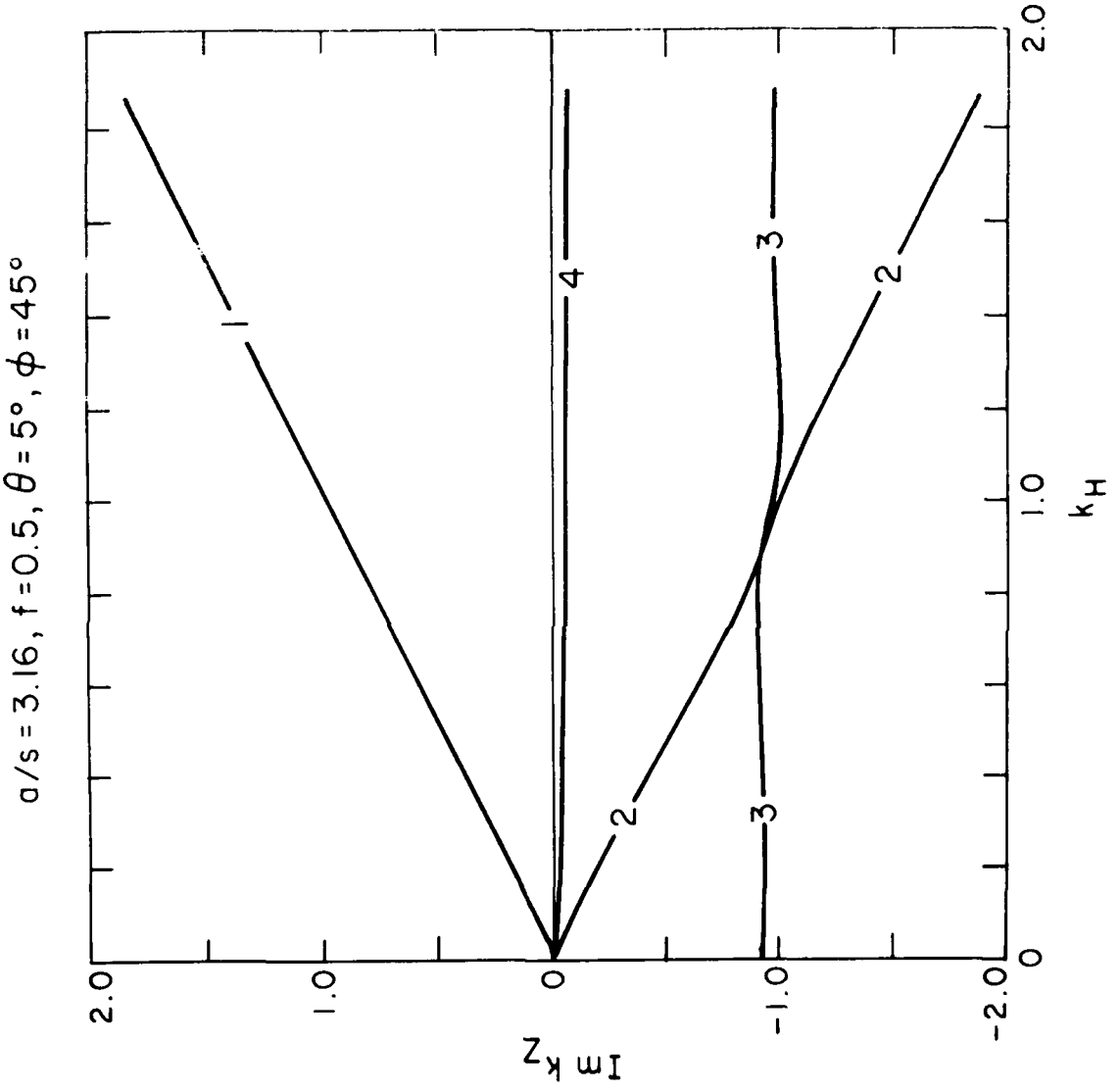

Figure 17b

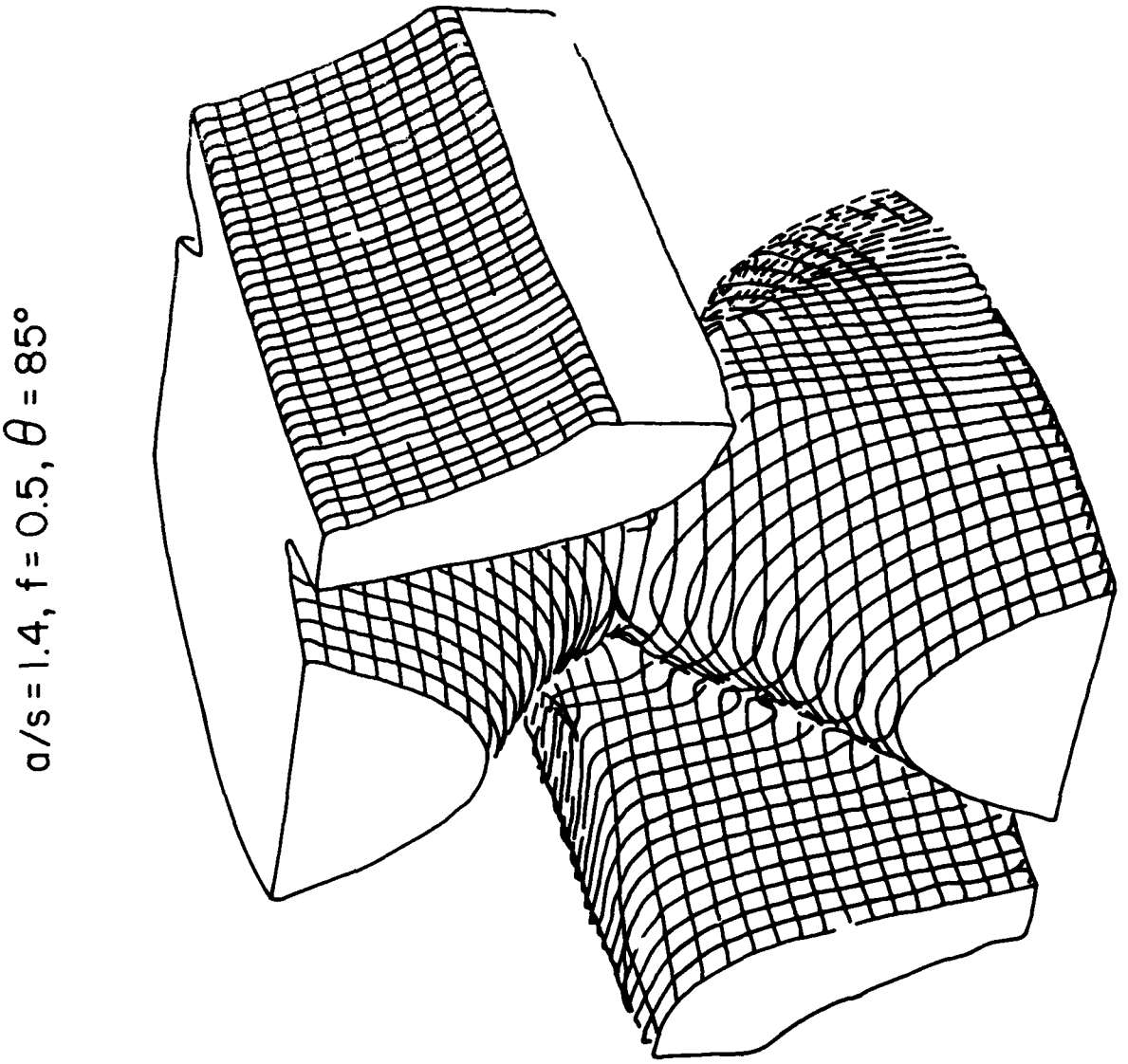

Figure 18

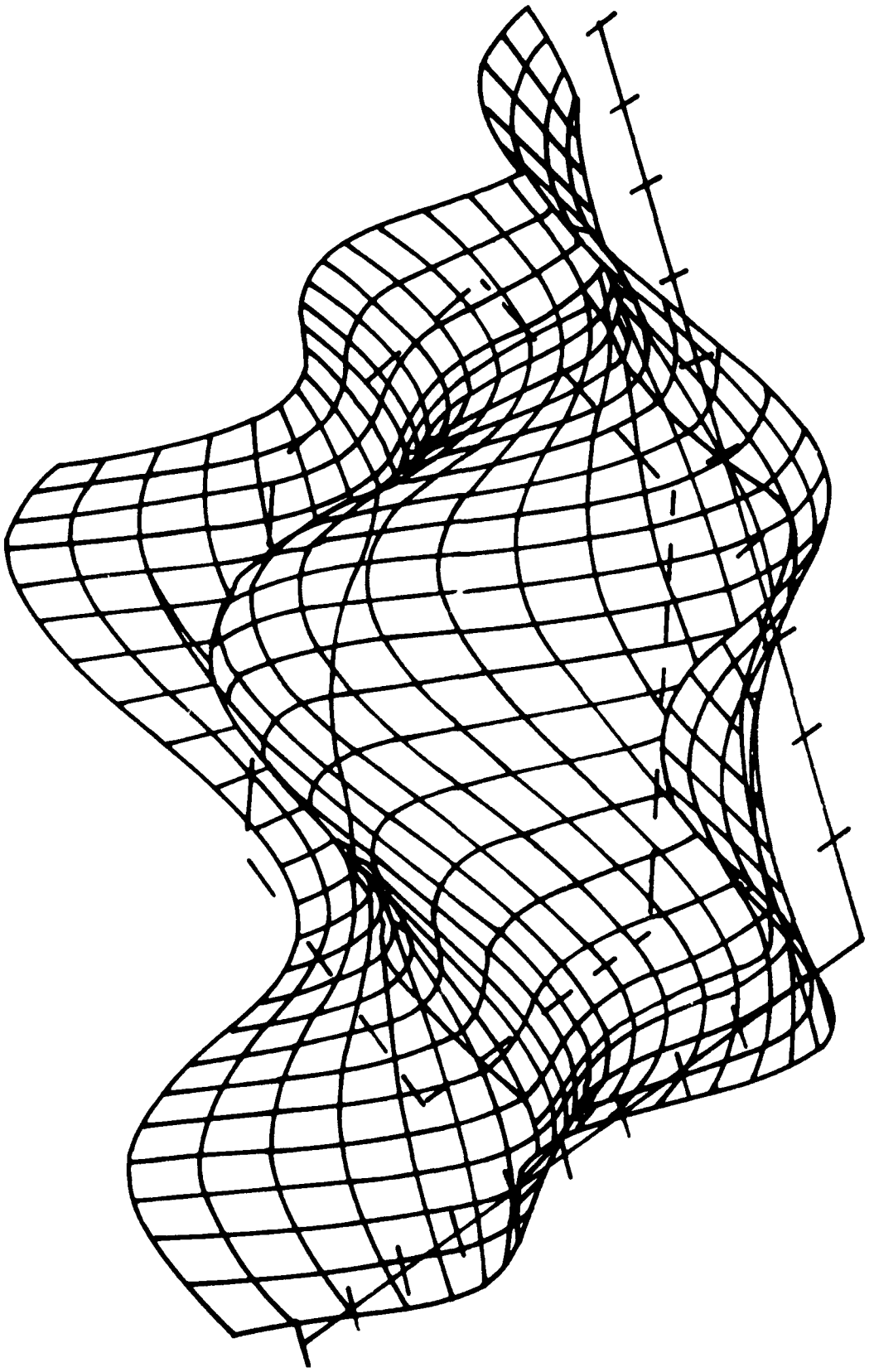

Figure 19

END

DATE
FILMED

8/

DTIC